Gene therapy using genetically modified lymphocytes targeting VEGFR-2 inhibits the growth of vascularized syngenic tumors in mice

Dhanalakshmi Chinnasamy,[1] Zhiya Yu,[1] Marc R. Theoret,[1] Yangbing Zhao,[1,2] Rajeev K. Shrimali,[1] Richard A. Morgan,[1] Steven A. Feldman,[1] Nicholas P. Restifo,[1] and Steven A. Rosenberg[1]

[1]Surgery Branch, National Cancer Institute (NCI), Clinical Research Center, Bethesda, Maryland, USA. [2]Department of Pathology and Laboratory Medicine, Abramson Family Cancer Research Institute, University of Pennsylvania, Philadelphia, Pennsylvania, USA.

Immunotherapies based on adoptive cell transfer are highly effective in the treatment of metastatic melanoma, but the use of this approach in other cancer histologies has been hampered by the identification of appropriate target molecules. Immunologic approaches targeting tumor vasculature provide a means for the therapy of multiple solid tumor types. We developed a method to target tumor vasculature, using genetically redirected syngeneic or autologous T cells. Mouse and human T cells were engineered to express a chimeric antigen receptor (CAR) targeted against VEGFR-2, which is overexpressed in tumor vasculature and is responsible for VEGF-mediated tumor progression and metastasis. Mouse and human T cells expressing the relevant VEGFR-2 CARs mediated specific immune responses against VEGFR-2 protein as well as VEGFR-2–expressing cells in vitro. A single dose of VEGFR-2 CAR-engineered mouse T cells plus exogenous IL-2 significantly inhibited the growth of 5 different types of established, vascularized syngeneic tumors in 2 different strains of mice and prolonged the survival of mice. T cells transduced with VEGFR-2 CAR showed durable and increased tumor infiltration, correlating with their antitumor effect. This approach provides a potential method for the gene therapy of a variety of human cancers.

Introduction

Most solid tumors (1, 2) and some hematologic malignancies (3) are characterized by an angiogenic phenotype that is an absolute requirement for tumor survival, progression, and metastasis (4, 5). Therapeutic approaches targeting molecules involved in tumor angiogenesis can inhibit tumor growth. Proliferating endothelial cells in the vessels within solid tumors aberrantly express high levels of angiogenic growth factors, receptors (6), and adhesion molecules (7) that are absent or barely detectable in established blood vessels, which are normally quiescent (5, 7). Among these, VEGF and its receptors appear to be the dominant regulators of angiogenesis responsible for the vascularization of normal and neoplastic tissues (5, 8). Overexpression of VEGF and its receptors is associated with tumor angiogenesis, survival, invasion, metastasis, recurrence, and prognosis in human cancers (6). VEGF stimulates angiogenesis mainly through VEGFR-2 (also known as Flk1 in mice and KDR in humans), a tyrosine kinase receptor that is overexpressed in tumor endothelial cells and on some tumor cells (3, 9). Pharmacologic approaches to inhibit VEGF, using monoclonal antibodies or small molecules, are of value in cancer treatment, though the cytostatic rather than cytotoxic nature of these interventions and the redundancy of angiogenic pathways have limited the curative potential of these treatments (2, 10–13).

Several immunotherapeutic approaches targeting VEGFR-2 on endothelial cells have been used to inhibit pathologic angiogenesis and tumor growth in animal models, which include neutralization of VEGFR-2 (14–19), immunization against VEGFR-2 (20–25), and coupling of VEGF to toxins to target and destroy VEGFR-2–expressing cells (26, 27) as well as disruption of *VEGFR* genes (28–30). Results in murine models targeting VEGFR-2 have been modest, though few evaluations have been performed in humans. In a recent paper evaluating the administration of anti–VEGFR-2 antibody to patients with cancer, partial responses were seen in 4 out of 27 patients (31).

Recent studies in experimental tumor models and humans demonstrated the effectiveness of adoptive cell therapy (ACT) in cancer treatment. Passive transfer of activated T cells targeting tumor antigens mediated the inhibition of large established tumors in mice (32) and objective cancer regression in 50%–70% of patients with metastatic melanoma (33–35). Recently, the ability to genetically modify lymphocytes by transduction of genes encoding conventional or chimeric T cell receptors has opened new possibilities for the application of ACT in cancer treatment (36–38).

An alternative to the use of conventional T cell receptors is the use of chimeric antigen receptors (CARs). These CARs are constructed by attaching the variable regions of an antibody as a single chain attached to T cell intracellular signaling chains to produce a molecule that when transduced into lymphocytes enables the cell to recognize targets based on the antigen recognition of the antibody. The availability of monoclonal antibodies against VEGFR-2 and the antitumor potency of ACT suggested that the transduction of a chimeric receptor recognizing VEGFR-2 into lymphocytes could produce self-replicating T cells capable of selectively destroying tumor vasculature.

In this study, we demonstrate that an ACT strategy, using a single dose of T cells engineered with a CAR comprising a single chain variable fragment (ScFv) antibody against mouse VEGFR-2 (the DC101 antibody, Imclone Systems Inc.) linked to intracellular mouse T cell

Conflict of interest: The authors have declared that no conflict of interest exists.
Citation for this article: *J Clin Invest.* 2010;120(11):3953–3968. doi:10.1172/JCI43490.

signaling domains, results in potent tumor treatment in 5 different syngeneic mouse tumor models in 2 different mouse strains. Further, to translate our preclinical findings to the treatment of human cancer, we have generated retroviral vectors expressing CAR, using ScFv derived from a fully human antibody against human VEGFR-2 (KDR1121, Imclone Systems Inc.), and tested their functional competency in vitro. VEGFR-2 CAR-modified human T cells generated robust immune responses against VEGFR-2 protein as well as cultured primary human endothelial cells expressing VEGFR-2, sparing other normal cell types. Overall, our preclinical findings provide the rationale for the application of this vascular targeting ACT strategy to the treatment of human cancer.

Results

Construction and expression of DC101-CAR–encoding retroviral vectors. We generated a series of MSGV-based recombinant retroviral vectors encoding a CAR comprising the ScFv of an anti-mouse VEGFR-2 antibody, DC101, linked to the intracellular mouse T cell signaling sequences, derived from the mouse CD28, 4-1BB molecules, and CD3-ζ chains via the mouse CD8 hinge and transmembrane regions (DC101-CD828BBZ). We also constructed a vector lacking the 4-1BB signaling domain (DC101-CD828Z), a vector retaining the DC101 ScFv sequence but lacking the intracellular T cell signaling sequences (DC101-CD8), a vector encoding a ScFv directed against a synthetic hapten TNP (SP6-CAR), and a vector lacking any of the CAR sequences (empty vector). These recombinant retroviral constructs are schematically represented in Figure 1A.

Surface expression of the retrovirally encoded transgene products in transduced $CD3^+$ primary mouse T cells was determined by flow cytometry using the soluble mouse VEGFR-2/human IgG-Fc fusion protein and PE-conjugated anti-human IgG-Fc. The DC101-CAR–expressing vectors efficiently and consistently transduced ConA/IL-7–activated mouse T cells (range 79%–86%), which were mostly (~90%) $CD8^+$ at day 5 after transduction, though both $CD4^+$ and $CD8^+$ cells exhibited similar CAR expression profiles (Figure 1B and Supplemental Table 1; supplemental material available online with this article; doi:10.1172/JCI43490DS1). The intensity of CAR expression derived from the DC101-CAR containing the 4-1BB signaling moiety was consistently lower than that derived from vectors lacking the 4-1BB sequence in all transduction experiments (Figure 1B and Supplemental Table 1).

DC101-CAR–modified mouse T cells are effective in generating antigen-specific immune responses in vitro. Proliferation and cytokine secretion by T cells in response to a target antigen is important in the activation and maintenance of an antigen-specific immune response. Therefore, we tested the ability of transduced cells to proliferate and secrete IFN-γ as an indicator of T cell response using several in vitro assays. First, we assessed the ability of DC101-CAR–engineered T cells to respond to immobilized VEGFR-2 protein. While there were no differences among T cells transduced with various vectors to respond to immobilized anti-mouse CD3 antibody, only the T cells engineered with DC101-CAR containing intact intracellular signaling sequences responded specifically to plate-bound target VEGFR-2 protein, as measured by proliferation (Figure 1C) and IFN-γ secretion (Figure 1D). Further, the presence of 4-1BB signaling sequences in the vector configuration had no impact on these in vitro functions of the DC101-CAR–transduced T cells.

Next, we determined whether DC101-CAR–modified T cells could specifically recognize mouse cell lines expressing VEGFR-2. Mouse endothelial cell lines and tumor lines from various tissue origins were examined for cell surface expression of VEGFR-2 by flow cytometry, using 2 different rat anti-mouse VEGFR-2 antibodies, with similar results, as shown in Figure 2A and Supplemental Figure 1A. The level of VEGFR-2 expression varied among the cell lines tested. While all transformed mouse endothelial cell lines (SVEC4-10EHR1, bEND.3, SVR, and MS1) showed high levels of VEGFR-2 expression, most of the cell lines showed either low (MC38, CT26, 4T1, and MCA205) or undetectable levels (MC17-51, B16-F10, RENCA, C4198, MB49, and NIH-3T3) of cell surface VEGFR-2 protein (Figure 2A and Supplemental Figure 1A). Two of the VEGFR-2–negative cell lines, MB49 and NIH-3T3, were stably transduced with a lentiviral vector expressing VEGFR-2 (MB49-Flk1 and 3T3-Flk1) and were used as positive controls in subsequent in vitro T cell functional assays.

A representative experiment showing the MHC-nonrestricted IFN-γ secretion of mouse T cells engineered to express DC101-CAR is presented in Figure 2B. DC101-CAR–transduced T cells specifically released IFN-γ in response to most of the VEGFR-2–positive cell lines tested, and the amount of IFN-γ secretion correlated highly with the level of VEGFR-2 expressed on target cells (Figure 2B, inset). Reactivity was restricted to T cells expressing DC101-CAR containing intact T cell signaling domains, and there were no significant differences in the performance of DC101-CAR, with or without 4-1BB signaling sequences in any of the in vitro functional assays tested. The specificity of the target antigen recognition was further confirmed by antibody blocking experiments. As shown in Supplemental Figure 1B, the anti–VEGFR-2 antibody DC101 blocked the recognition of DC101-CAR–transduced T cells against $VEGFR\text{-}2^+$ endothelial bEND.3 and MB49-Flk-1 tumor cell lines, while no blocking was observed either with an anti-mouse VEGFR-1 or isotype control antibodies.

Consistent with these results, in cytotoxicity assays, the DC101-CAR–modified T cells specifically lysed the VEGFR-2–positive target cells but not the VEGFR-2–negative cell types. Whereas, the mock, empty vector, or SP6-CAR–transduced T cells were unable to lyse any of the target cells tested (Figure 3).

Impact of DC101-CAR–engineered T cells on established tumors in syngeneic mice. To determine the therapeutic efficacy of our tumor vasculature targeting strategy, DC101-CAR–transduced cells were used to treat syngeneic mice bearing established vascularized subcutaneous tumors. Unless otherwise noted, mice in all treatment groups received 2 daily doses of exogenous recombinant human IL-2 (rhIL-2) for 3 days, beginning with the first day of T cell therapy.

As shown in Figure 4A, T cells expressing the DC101-CAR were capable of mediating a significant growth inhibitory effect against several weakly immunogenic tumors, including B16-F10 ($P = 0.009$), MC38 ($P = 0.009$), MCA205 ($P = 0.025$), CT26 ($P = 0.009$), and RENCA ($P = 0.008$) tumors in syngeneic mice. Further, in vivo tumor treatment studies conducted in C57BL/6 mice bearing B16-F10 tumors revealed that a single dose of DC101 antibody (Figure 4B), or transfer of T cells expressing DC101 ScFv but lacking the intracellular T cell signaling molecules (Figure 4C), had no effect on controlling the tumor growth. In addition, mice treated with IL-2 alone (Figure 4, A and B) or with T cells engineered with an irrelevant CAR (SP6-CAR) or an empty vector failed to induce tumor inhibition (Figure 4C). The treatment effect of DC101-CAR–transduced T cells against the B16-F10 melanoma was a direct function of the number of cells administered (Figure 4D). Delay in tumor growth was achieved with as few as 2×10^6 DC101-CAR–transduced T cells ($P = 0.008$).

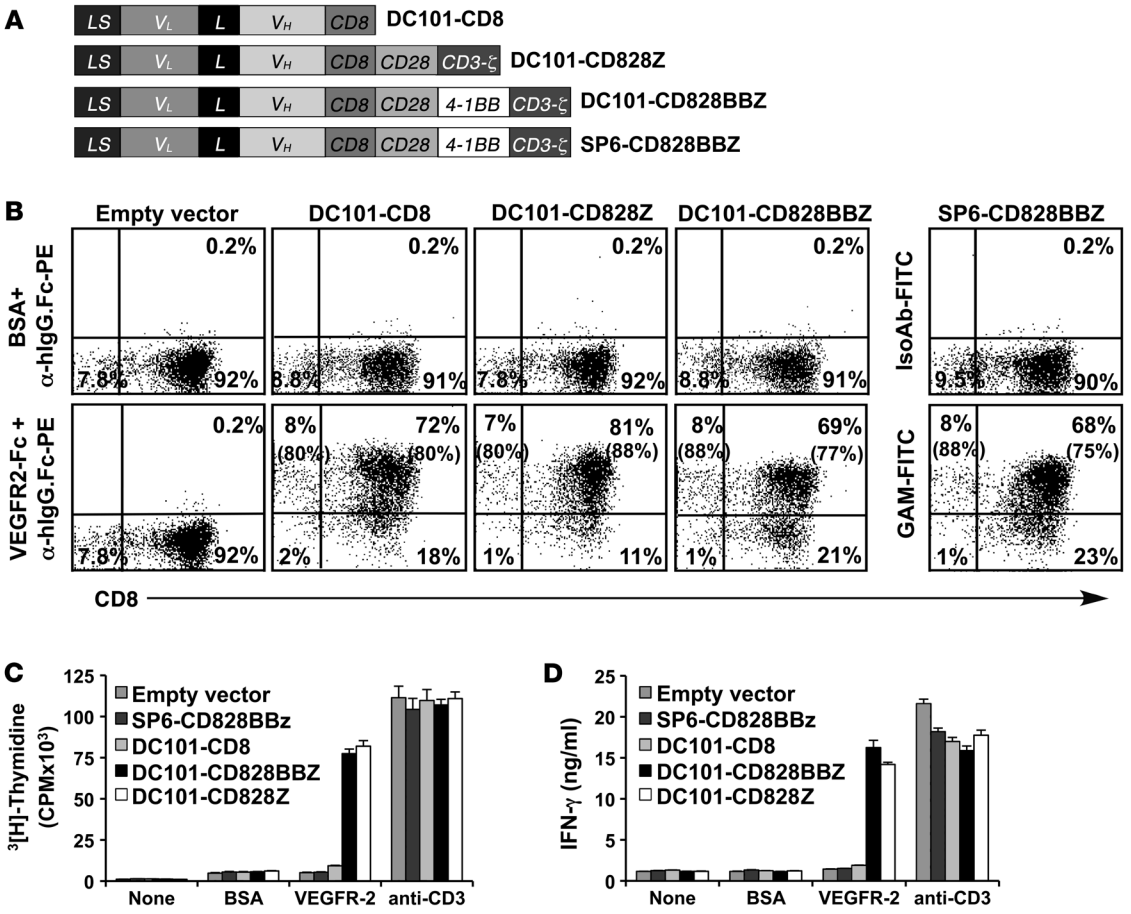

Figure 1

Construction and characterization of recombinant retroviral vectors expressing CARs targeted against mouse VEGFR-2. (**A**) Schematic representation of recombinant retroviral vectors encoding CARs used in this study. In the DC101-CD828BBZ CAR vector, the DC101 ScFv is made up of the V_H and V_L derived from a rat IgG against mouse VEGFR-2 joined by a 218 linker that is linked to the hinge and transmembrane regions of the mouse CD8α chain and mouse intracellular signaling sequences derived from CD28, 4-1BB, and CD3-ζ molecules. The DC101-CD828Z vector lacked the 4-1BB signaling domain. The DC101-CD8 construct lacked all the intracellular signaling sequences. The SP6-CD828BBZ construct was derived from SP6, a mouse monoclonal antibody raised against a hapten 2, 4, 6-trinitrophenyl (TNP). (**B**) Enriched splenic CD3+ T cells were transduced with indicated retroviral vectors shown in **A**. Four days after transduction, cells were analyzed for transgene expression by flow cytometry. Representative FACS data are presented, showing the percentage of T cells in each quadrant, with the percentage of transgene-positive cells in parentheses. IsoAb, isotype control antibody. GAM, goat anti-mouse antibody. (**C** and **D**) Enriched CD3+ mouse T cells were transduced with the indicated retroviral vectors. Four days later, cells were cultured on antigen-coated 96-well microtiter plates for 3 days. (**C**) The proliferation of T cells was measured as [3H]thymidine incorporation during the last 16 hours. (**D**) Culture supernatants were assayed for IFN-γ by ELISA. Results are presented as the mean ± SEM of triplicates.

In most of the tumor treatment studies with a single dose of 2×10^7 DC101-CAR–modified T cells, there was a rapid inhibition of tumor growth over a period of 2–3 weeks; during this remission period, the parental tumor became necrotic and fibrous, but tiny nodules of viable tumor reappeared at the periphery of the parental tumor and eventually regenerated in many mice. However, effective tumor treatment and tumor-free survival was achieved in mice bearing established B16-F10 or MCA205 tumors, treated with 3 sequential weekly doses of 5×10^6 DC101-CAR–transduced T cells and rhIL-2 (Figure 5). Studies are underway to further improve the efficacy of this antiangiogenic cell therapy strategy to obtain complete tumor destruction or to limit the transition of the tumor to a quiescent or anergized state.

Impact of 4-1BB on antitumor activity and in vivo persistence of adoptively transferred DC101-CAR–transduced T cells. T cells transduced with DC101-CAR vector, either containing (DC101-CD828BBZ) or lacking (DC101-CD28Z) the 4-1BB intracellular signaling sequences, performed equally well and were statistically indistinguishable ($P = 0.1$) in delaying the growth of established, bulky B16-F10 tumors (Figure 6A). While T cells transduced with either of the vectors evoked a moderate antitumor effect in the absence of exogenous IL-2, their tumor inhibitory effect was significantly enhanced by coadministration of rhIL-2 ($P = 0.004$ and $P = 0.009$, respectively; Figure 6A).

To determine the impact of 4-1BB signaling on the long-term persistence of CAR-modified T cells in vivo, B16 tumors from 2 mice from each of the treatment groups that received DC101-CAR-engineered T cells and rhIL-2 (from experiment shown in Figure 6A) were harvested at 30 days after T cell transfer and individually analyzed for the presence of DC101-CAR–expressing T cells by flow cytometry (Figure 6B). Mice treated with DC101-CD828BBZ CAR-engineered T cells had 4- to 5-fold more DC101-CAR–expressing CD3+ in the tumor than mice treated with T cells carrying

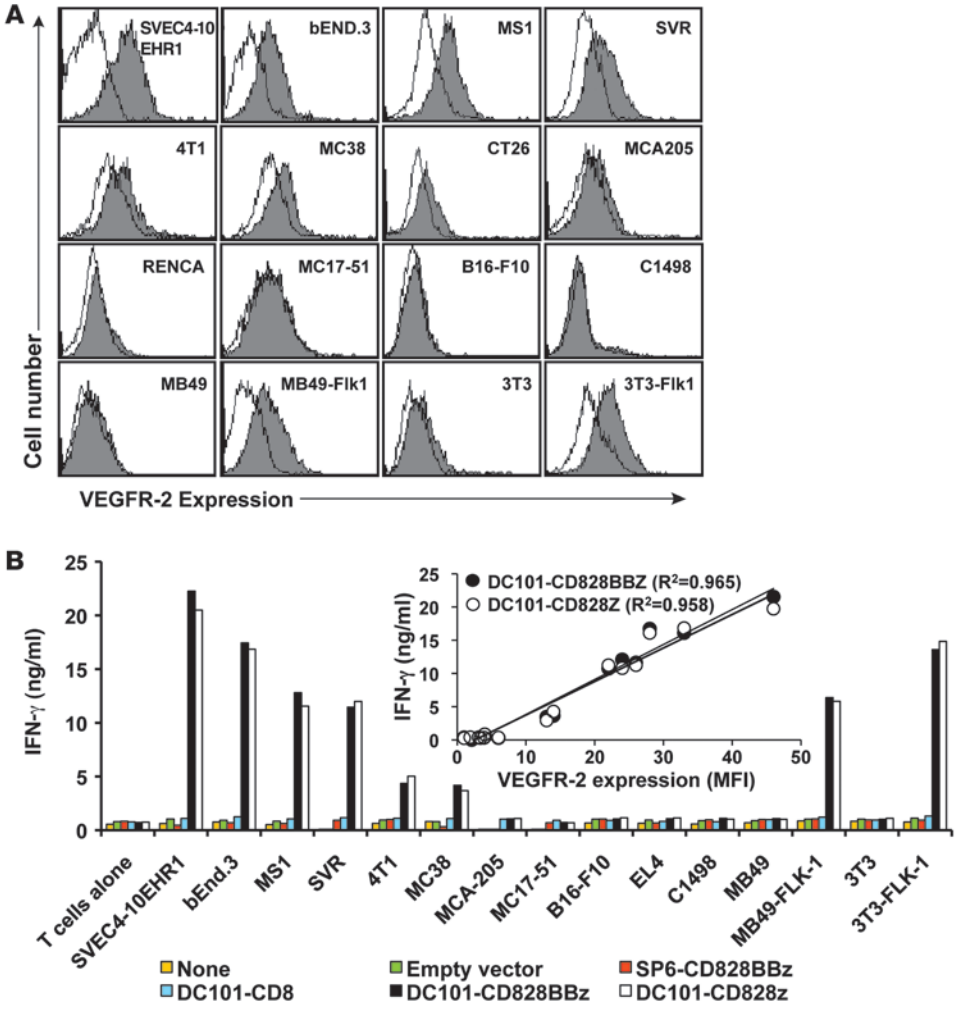

Figure 2
DC101-CAR–transduced mouse T cells are functionally competent in generating immune responses against VEGFR-2–expressing mouse cell lines. (**A**) Expression of VEGFR-2 on mouse endothelial cells and tumor cells. Indicated mouse cell lines were incubated sequentially with recombinant DC101 antibody (a rat IgG antibody specific to mouse VEGFR-2) or isotype control rat IgG1, soluble mouse VEGFR-2–hIgG-Fc protein, and PE-labeled anti-hIgG-Fc (α-hIgG.Fc) and analyzed by FACS. Filled histogram, VEGFR-2–specific staining; open histogram, staining with rat IgG1. Results shown are representative of 2 experiments. (**B**) Primary mouse T cells were transduced with various retroviral vector constructs shown in Figure 1A. Four days later, cells were cocultured with the indicated mouse cell lines. Culture supernatants harvested at 24 hours after coculture were assayed for IFN-γ by ELISA. Results are presented as the mean of triplicate wells. Correlation between the IFN-γ secretion of DC101-CAR–engineered effector T cells and the MFI of VEGFR-2 expression on the target cells is shown (inset).

DC101-CD828Z CAR that lacked 4-1BB. These results suggest that 4-1BB influenced the persistence of adoptively transferred antigen-specific T cells at the tumor site. Thus, in subsequent experiments, we used the DC101-CD828BBZ vector.

Impact of host lymphodepletion on the therapeutic efficacy of adoptive therapy with DC101-CAR–transduced T cells. Depletion of host immune cells prior to adoptive cell transfer can enhance the antitumor efficacy of transferred antigen-specific T cells by eliminating immune suppressor cells as well as lymphocytes that compete with the transferred cells for homeostatic cytokines (39, 40). Therefore, in all of the previous adoptive T cell therapy experiments, mice received 5 Gy total body irradiation (TBI) prior to cell transfer. Irradiation, however, could potentially adversely alter or damage tumor vasculature and/or skew the expression of the target antigen, VEGFR-2. Therefore, we tested the in vivo antitumor activity of DC101-CAR–engineered T cells in mice, with or without host lymphodepletion prior to adoptive T cell transfer (Figure 6C). Consistent with the findings from our previous experiments, the DC101-CAR–expressing T cells reproducibly generated an antitumor response in lymphodepleted mice compared with those engineered with SP6-CAR or empty vector ($P = 0.009$). The tumor inhibitory effect was statistically indistinguishable between the treatment groups that received DC101-CAR T cells, either in the presence or absence of host preconditioning with irradiation ($P = 0.251$).

DC101-CAR–transduced T cells efficiently traffic to tumor and specifically accumulate in tumor. Trafficking of effector T cells to the tumor site is one of the important factors that can affect tumor treatment using adoptively transferred T cells. To determine the extent and kinetics of trafficking of DC101-CAR T cells to tumor, we harvested tumors and spleens from mice treated with either empty vector- or DC101-CAR–transduced Thy1.1$^+$ T cells at various times after adoptive therapy and performed flow cytometric analysis. The percentage of infused T cells that specifically expressed Thy1.1 in the total population of single cell preparations of spleen and the lymphocyte-gated population of cells from tumor was determined. Representative FACS data (Figure 7A) and pooled data were obtained from 3 different mice from independent experiments (Figure 7B). By day 3, adoptively transferred T cells trafficked similarly to spleen and tumor irrespective of their genetic modification. However, at days 6 and 9, trafficking to the tumor was greater for the DC101-CAR–endowed T cells. These findings were confirmed by direct visualization of adoptively transferred Thy1.1$^+$ T cells, after staining the tumor sections with Thy1.1 specific antibody. Consistent with these data, tumor samples taken on day 4 after cell transfer from mice treated with DC101-CAR–transduced Thy1.1$^+$ T cells contained more Thy1.1$^+$ T cells than those treated with empty vector-transduced cells (Figure 7C). At this time point, the tumor vessels contained

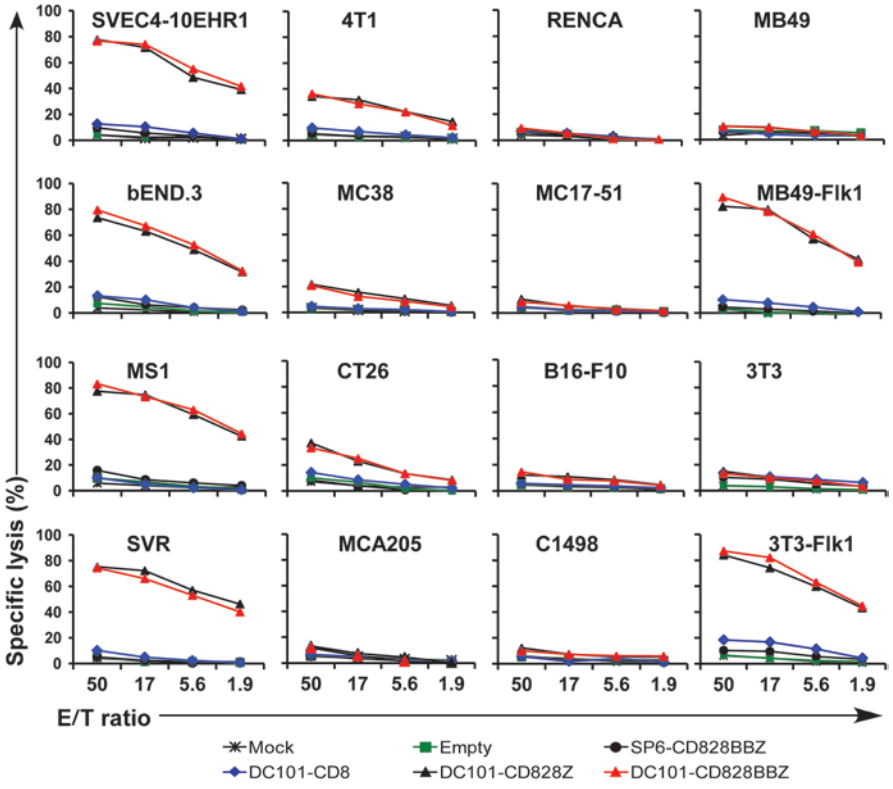

Figure 3
Primary mouse T cells modified to express VEGFR-2 CAR specifically lyse mouse cells expressing VEGFR-2. Primary mouse T cells, mock transduced with an empty or CAR-expressing retroviral vector as indicated in the figure, were incubated with the target cells shown in the figure at varying effector-to-target (E/T) ratios, and cell lysis was determined by using the standard Cr^{51} release assay. Each data point reflects the mean of triplicates.

DC101-CAR–transduced T cells in close association with endothelial cells in the tumor vessels (Figure 7D). Furthermore, tumor sections stained with the endothelial cell marker CD31 revealed a reduced number of vessels in the tumors of mice treated with DC101-CAR–transduced T cells compared with those treated with empty vector-transduced T cells (Figure 7E).

The enhanced trafficking and increase in numbers of DC101-CAR–transduced T cells in the tumor seem to be the consequence of in vivo target antigen engagement, rather than the result of any intrinsic differences in antigen-independent mechanisms, such as increased expression of chemokine receptors when comparing CAR-transduced and empty vector-transduced T cells. There were no differences between expression levels of chemokine receptors CCR7, CCR9, CXCR-3, and CXCR-4 as well as the homing molecule L-selectin (CD62L), which are known to be involved in the trafficking of T cells, when comparing T cells transduced with retroviral vectors expressing DC101-CD828BBZ, DC101-CD828Z, SP6-CD828BBZ, or no transgene (Supplemental Figure 3).

Toxicity resulting from the administration of CAR expressing VEGFR-2. In all of our tumor treatment studies, performed in a total of 135 mice C57BL/6 mice bearing established subcutaneous tumors of different histologies, the adoptively transferred syngeneic T cells contained greater than 90% $CD8^+$ T cells. No treatment related morbidity or mortalities were documented in those mice that received 5 Gy TBI, up to 2×10^7 T cells transduced with either DC101-CD828BBZ or DC101-CD828Z CAR, and high-dose IL-2. Histopathologic analysis of various organs in C57BL/6 mice treated with maximum numbers (2×10^7 T cells) of VEGFR-2 CAR-modified T cells showed no evidence of treatment related toxicity, despite reports of low levels of VEGFR-2 expression in vascularized tissues, such as kidney (41–43), retina (41), and pancreas (44).

In contrast, severe toxicity was seen in tumor-bearing BALB/c mice treated similarly with 2×10^7 DC101-CAR–transduced syngeneic T cells. However, in BALB/c mice with established CT26 or RENCA tumors, comparable antitumor effects were achieved without any treatment related toxicities if the number of administered T cells was reduced to 5×10^6 or by administering 2×10^7 purified syngeneic $CD8^+$ T cells transduced with DC101-CAR (Supplemental Figure 4A). Histopathologic analysis of BALB/c mice treated with 2×10^7 DC101-CAR–transduced T cells and IL-2 revealed findings characteristic of cytokine-induced hypotension, including multifocal mild coagulation necrosis in the liver, mild hepatic pericholangitis, and pulmonary perivasculitis and villous atrophy, villous blunting, and crypt epithelial hyperplasia of the small intestine and colon. No abnormalities in the gross appearance of the heart, lungs, liver, kidneys, spleen, pancreas, uterus, ovaries, or brain were seen.

The differences in toxicity seen in C57BL/6 mice compared with those in BALB/c mice were apparently due to the increased numbers of $CD4^+$ T cells present in the final cell product used in adoptive transfer. Although the $CD3^+$ T cells obtained from BALB/c spleens were cultured similarly to those of the C57BL/6 mice, the final BALB/c cell product (cultured for 5–6 days) contained approximately 60% $CD8^+$ T cells and 40% $CD4^+$ T cells at the time of adoptive transfer. No toxicity was seen in BALB/c mice (in 3 independent experiments, involving 15 tumor-bearing mice) treated with reduced numbers of unseparated T cells (5×10^6) or 2×10^7 purified $CD8^+$ T cells transduced with DC101-CAR, while mice receiving 2×10^7 DC101-CAR–modified T cells, containing both $CD8^+$ T cells (~60%) and $CD4^+$ (~40%) T cells, showed morbidity and mortality in the same experiment, as shown in Supplemental Figure 4A. These findings were further evaluated in B16 tumor-bearing C57BL/6 mice, in which morbidity and mortalities were evidenced if the mice were treated with purified $CD4^+$ T cells

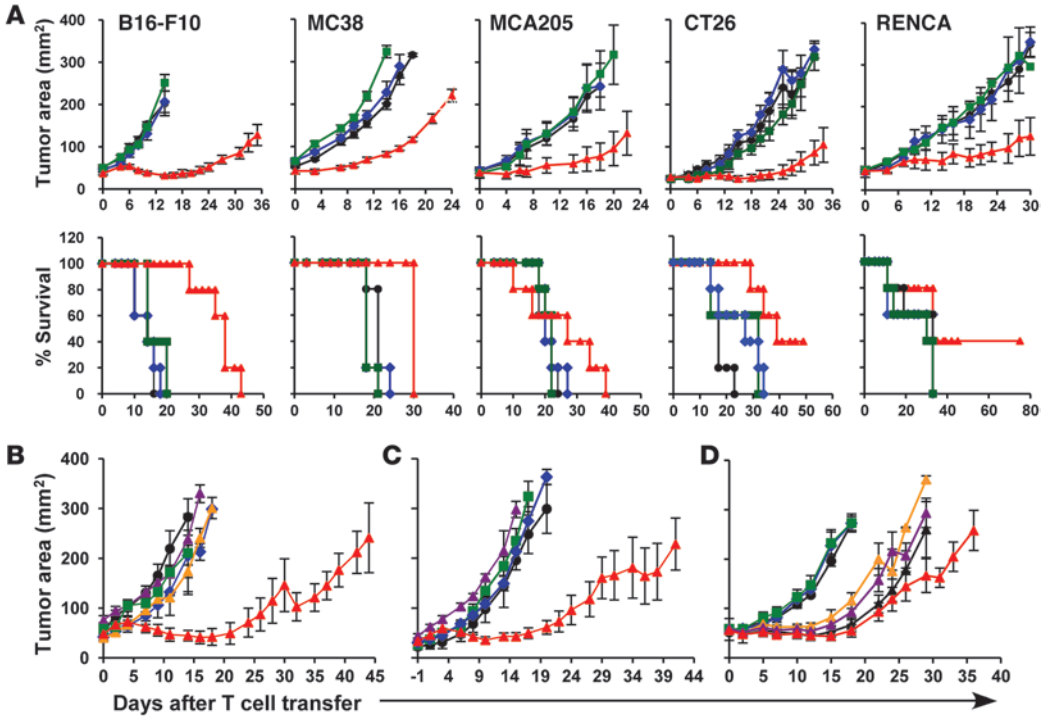

Figure 4
Adoptively transferred DC101-CAR–engineered mouse T cells inhibit multiple types of established syngeneic tumors in vivo. (**A**) Mice bearing established subcutaneous tumors were sublethally irradiated at 5 Gy TBI and treated with 2 × 10^7 DC101-CD828BBZ–transduced (red triangles) or empty vector–transduced (green squares) syngeneic mouse T cells in conjunction with rhIL-2. Control groups received rhIL-2 alone (blue diamonds) or no treatment (black circles). Mice bearing CT26 or Renca tumors were treated with 5 × 10^6 T cells. (**B**) The antitumor effect of DC101-CAR–transduced T cells was cell mediated and not due to an antibody effect. C57BL/6 mice bearing subcutaneous B16-F10 tumors were treated as described in **A**. One group in this experiment received a single dose of 800 μg/mouse DC101 (orange triangles) or rat IgG1 (purple triangles) antibodies plus rhIL-2. (**C**) C57BL/6 mice bearing subcutaneous B16-F10 tumors were treated with T cells transduced with DC101-CAR (red triangles) or SP6-CAR vector (blue diamonds), containing intact mouse intracellular signaling sequences, 28BBZ, DC101-CD8 vector that lacked all the signaling domains (purple triangles), or an empty vector (green squares) plus rhIL-2, or were untreated (black circles). (**D**) C57BL/6 mice bearing B16-F10 tumors were treated with 2 × 10^7 (red triangles), 1 × 10^7 (black triangles), 5 × 10^6 (purple triangles), or 2 × 10^6 (orange triangles) syngeneic T cells transduced with DC101-CD828BBZ plus rhIL-2. Control groups received 2 × 10^7 T cells transduced with an empty vector plus rhIL-2 (green squares), rhIL-2 alone (blue diamonds), or received no treatment (black circles). Each treatment group included a minimum of 5 mice. Serial, blinded tumor measurements were obtained, and the products of perpendicular diameters were plotted ± SEM.

transduced with VEGFR-2 CAR or 2 × 10^7 T cells containing a 1:1 mixture of 1 × 10^7 purified $CD8^+$ and 1 × 10^7 $CD4^+$ T cells, both transduced with CAR. Whereas, effective tumor treatment was achieved with no adverse effects in mice treated with either 2 × 10^7 unseparated $CD3^+$ T cells (>90% $CD8^+$ T cells) or purified $CD8^+$ T cells transduced with VEGFR-2 CAR (Supplemental Figure 4B).

Importantly, in multiple experiments, treatment of non-tumor-bearing BALB/c or C57BL/6 mice with 2 × 10^7 CAR-transduced T cells containing equal numbers of $CD4^+$ and $CD8^+$ T cells was well tolerated, with no adverse effect or toxicities (data not shown). Taken together, these findings suggest that the cause of these toxicities observed with the adoptively transferred VEGFR-2 CAR-transduced T cells was restricted to the $CD4^+$ T cell recognition of the target antigen VEGFR-2 in the tumor vascular network and subsequent downstream molecular events, rather than their off-target cell-mediated cytotoxicities to normal vessels or tissues.

Construction and testing of retroviral vectors expressing CAR against human KDR. We next explored the translation of our preclinical findings to the treatment of human tumors. We constructed a set of recombinant retroviral vectors expressing CAR against the human VEGFR-2 (KDR). The first KDR-CAR vector, referred to as KDR1121-hCD828BBZ, was composed of a ScFv derived from a fully human antibody, KDR1121 (45), specific to the human KDR antigen linked to the hinge and transmembrane sequences from the human CD8α, which was in turn fused to the intracellular sequences derived from the human CD28 (*CD28*), 4-1BB (*TNFRSF9*), and CD3-ζ (*CD247*) genes. A second vector, referred to as KDR1121-hCD28Z, was composed of KDR1121 ScFv linked to the hinge and transmembrane sequences and the intracellular signaling domain of the human CD28 molecule, followed by cytoplasmic sequences from CD3-ζ. The configuration and components of each of these vectors are illustrated in Figure 8A.

The functional integrity of these KDR-CAR–encoding retroviral vectors was tested in vitro in several assays. Supernatants from gibbon ape leukemia virus–pseudotyped high-titer virus producer cells were used to transduce anti-CD3–activated (OKT3-activated) human PBLs from 3 different donors. The KDR-CAR–encoding retroviral vectors efficiently transduced human $CD3^+$ T cells at a high frequency (85% ± 1.7% and 79% ± 1.5% [mean ± SEM, n = 5] for KDR1121-hCD28Z and KDR1121-hCD828BBZ vectors, respectively).

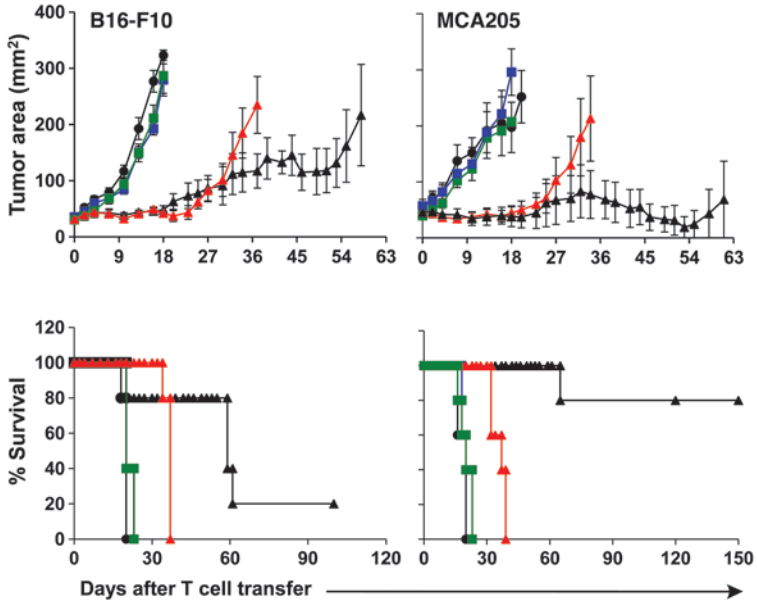

Figure 5
Adoptive transfer of multiple doses of DC101-CAR–transduced mouse T cells effectively controlled the tumor growth and increased the survival of tumor-bearing mice. Mice bearing established subcutaneous B16 or MCA205 tumors were sublethally irradiated at 5 Gy TBI and injected with a single dose of 2×10^7 DC101-CD28BBZ–transduced (red triangles) or empty vector–transduced (green squares) syngeneic mouse T cells, in conjunction with rhIL-2. Some groups received 3 sequential doses of 5×10^6 DC101-CAR–transduced (black triangles) or empty vector–transduced (blue squares) T cells at 7- to 10-day intervals and 2 daily doses of rhIL-2 for 3 days following cell transfer. The control group did not receive T cells or rhIL-2 (black circles). Each treatment group included a minimum 5 of mice. Serial, blinded tumor measurements were obtained, and the products of perpendicular diameters were plotted ± SEM.

Even though both vectors transduced the human PBLs at a comparable rate, the MFI of CAR expression driven from KDR1121-CD828BBZ vector possessing the 4-1BB signaling sequence was slightly lower (MFI of 160 ± 16 and 123 ± 21 for KDR1121-hCD28Z and KDR1121-hCD828BBZ vectors, respectively, $n = 5$), as shown in Figure 8B, a result similar to our findings with the DC101-CAR in mouse T cells (Figure 1B and Supplemental Table 1). However, no differences were seen between these 2 KDR-CAR vectors transduced into human T cells when measuring antigen-specific proliferation (Figure 8C) and IFN-γ secretion of cells (Figure 8D) in response to immobilized KDR protein in vitro.

Next, we tested the ability of KDR-CAR–modified T cells to recognize KDR-positive human cells, as measured by specific IFN-γ secretion. KDR1121-CD828BBZ and KDR1121-CD28Z CAR-transduced PBLs from 3 different donors, at 8 days after transduction, were cocultured for 24 hours with KDR-negative 293 cells or 293-KDR cells, a stable transfectant expressing KDR protein. Both vectors conferred similar levels of specificity and functionality to the transduced human T cells, as evidenced by their ability to specifically recognize only the KDR-expressing 293-KDR cells and not the 293 cells (Figure 8E). We also determined the activity of KDR1121-CD828BBZ vector–transduced T cells against various primary human cells. A panel of normal primary human endothelial and epithelial cells from different tissue origins, skin-derived fibroblasts, and muscle myoblasts cultured in vitro for a short period, were examined for KDR expression by flow cytometry. The KDR protein was readily detectable only in 293-KDR and cultured primary endothelial cells and not in any of the primary epithelial cells, skin-derived fibroblasts, and myoblasts tested (Figure 9A). The intensity of KDR expression was higher in skin-derived human dermal microvascular endothelial cells (HMVEC-D) compared with that of lung-derived human microvascular endothelial cells (HMVEC-L) or HUVECs. Notably, the KDR1121-hCD828BBZ CAR-transduced T cells secreted IFN-γ only in response to KDR-positive endothelial cells, irrespective of their tissue origin, and failed to recognize the other primary cells tested (Figure 9B). Consistent with these results, in cytotoxicity assays, the KDR1121-hCD828BBZ and KDR1121-hCD28Z CAR-modified T cells specifically lysed the KDR-positive target cells but not the KDR-negative cell types. Whereas, the mock- or SP6-CAR–transduced T cells were unable to lyse any of the target cells tested (Figure 9C).

Discussion

ACT immunotherapy designed to directly target antigens expressed on tumor cells can result in durable objective regression in patients with metastatic melanoma (32–35). Despite its demonstrated effectiveness in experimental mouse tumor models and in humans, the clinical application of ACT is limited because of the need to identify antigens with highly selective expression in cancer, escape of tumor cells from immune destruction by antigen modulation, decreased MHC expression by tumor cells, lack of costimulatory molecule expression on tumors, and other immunosuppressive mechanisms at the tumor site that impede extravasation and survival of T cells and dampening immune responses (46–50). Antiangiogenic approaches can potentially overcome many of these tumor-specific factors, though the cytostatic nature of the available treatments and the redundancy of angiogenic pathways have limited its effectiveness (10, 51). Redirecting immune cells to target tumor vasculature offers an alternative to overcome the obstacles confronting both conventional tumor-specific immunotherapy and the use of cytostatic antiangiogenic inhibitors, because of the potent effector functions of activated lymphocytes and the consistent expression of VEGFR-2 on tumor vasculature.

Prior attempts to combine immunotherapy and antiangiogenic therapy have largely involved attempts to directly immunize mice against tumor antigens, in conjunction with the administration of antiangiogenic agents (52, 53), or to directly immunize against receptors on tumor vasculature (20, 22–25, 54). The modest results in these studies largely resulted from the inability to adequately immunize the host against self-expressed tumors or vascular determinants. An alternate approach, using the combination of multiple infusions of cytotoxic T cells engineered to express VEGF sequences fused to intracellular signaling chains plus the administration of a conventional angiogenesis inhibitor TNP-470, delayed tumor growth in vivo in tumor models in mice (51).

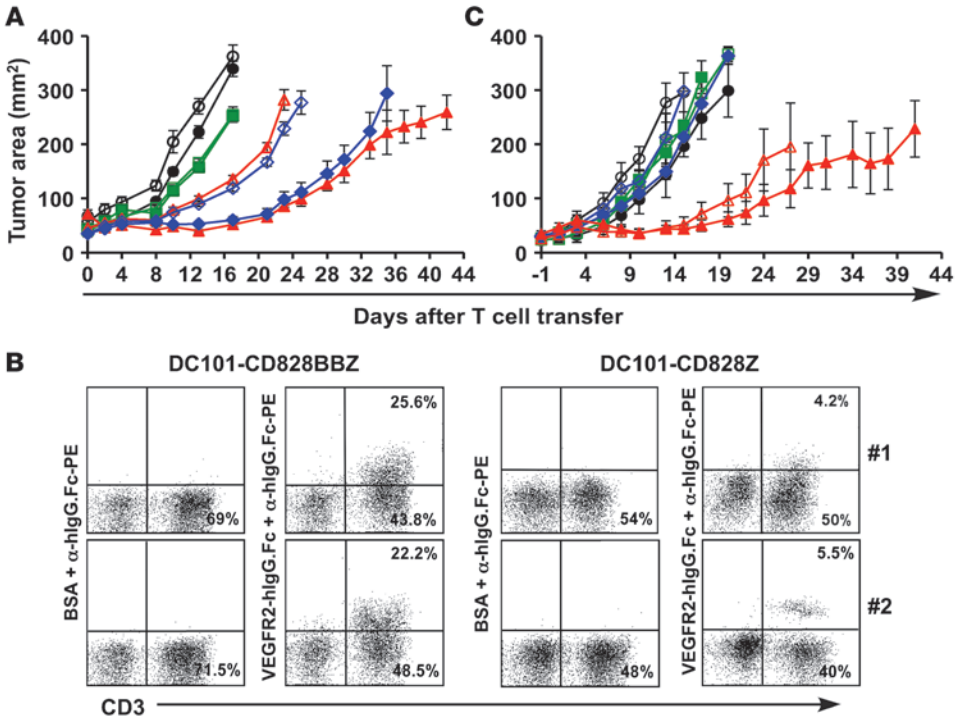

Figure 6

Impact of exogenous rhIL-2, 4-1BB signaling, and host lymphodepletion on tumor treatment effect of DC101-CAR–transduced T cells. (**A**) DC101-CAR–transduced T cells required exogenous rhIL-2 but not 4-1BB signaling for effective tumor treatment. C57BL/6 mice bearing subcutaneous B16-F10 tumors received 2×10^7 syngeneic T cells transduced with DC101-CAR containing the 4-1BB signaling domain (DC101-CD828BBZ, blue diamonds) or lacking 4-1BB (DC101-CD828Z; red triangles) or an empty vector (green squares). Control groups received no T cells (black circles). Groups represented by filled symbols received exogenous rhIL-2 administration, and those represented by open symbols did not receive rhIL-2. (**B**) 4-1BB signaling enhanced persistence of DC101-CAR–modified T cells in vivo. Tumor samples from 2 mice treated with DC101-CAR–transduced T cells plus rhIL-2, shown in Figure 4A, were harvested on day 30 after T cell transfer. The low-density cell fraction was prepared from tumor samples, and cell surface expression of DC101-CAR was determined by FACS. The percentage of $CD3^+$ T cells expressing DC101-CAR in the lymphocyte-gated region of the forward and side scatter profiles is shown in top right quadrants, and the percentage of $CD3^+$ T cells negative for DC101-CAR expression is shown in the bottom right quadrants. (**C**) Impact of host lymphodepletion on in vivo tumor therapeutic effect of DC101-CAR–engineered T cells. C57BL/6 mice bearing subcutaneous B16-F10 tumors received 2×10^7 syngeneic T cells transduced with DC101-CAR (red triangles), SP6-CAR (blue diamonds), or an empty vector (green squares) plus rhIL-2 or were not treated with T cells (black circles). Mice in groups represented by filled symbols received 5 Gy TBI prior to T cell transfer, and mice in groups represented by open symbols did not receive 5 Gy TBI. (**A** and **C**) Serial, blinded tumor measurements were obtained, and the products of perpendicular diameters were plotted ± SEM.

Here we have developed a cytotoxic ACT strategy to selectively destroy the tumor vasculature by using genetically modified T cells expressing a CAR against VEGFR-2, a signaling receptor that is overexpressed on tumor vascular endothelial cells. These cells are thought to be genetically stable nonmalignant cells and, unlike tumor cells, are unlikely to mutate into drug-resistant or antigen-loss variants (55, 56). The non-MHC-restricted antigen recognition potential of T cells expressing CARs could provide an opportunity to treat cancer patients independent of their HLA status.

We demonstrated a high frequency of transduction and a high level of expression of these transduced CARs in mouse and human T cells. These cells generated specific immune responses, upon stimulation by their predefined target antigen in vitro, that was highly correlated with the level of expression of VEGFR-2 on target cells. Mouse lymphocytes bearing a VEGFR-2–specific CAR were effective in treating all 5 vascularized syngeneic tumors of diverse histological origins tested, including the B16 melanoma, the MC38 colon adenocarcinoma, and the MCA-205 sarcoma in C57BL/6 mice as well as the CT26 colon carcinoma and the Renca renal cell carcinoma in BALB/c mice. The antitumor effect of VEGFR-2 targeting CAR-transduced T cells was strictly dependent on the presence of the intracellular T cell signaling domains in the CAR configuration, which provided evidence that the antitumor effect was cell mediated rather than solely an antibody-mediated cytotoxicity.

The antitumor effect of VEGFR-2 CAR appeared to be mediated through the destruction of VEGFR-2–expressing cells in the tumor vasculature and not due to their direct cytotoxicity on the tumor itself. The B16-F10 melanoma used in this study was negative for VEGFR-2 protein expression both in the cultured cell line (Figure 2A and Supplemental Figure 1A) and in the established tumors derived from these cells in vivo in mice (Supplemental Figure 2, A and B) as previously reported (24, 54). Furthermore, the CAR-modified T cells failed to generate antigen-specific IFN-γ response and lytic activity against B16-F10 melanoma cells in vitro. Our efforts to date to directly observe the in vivo destruction of tumor vasculature through measurements of micro vessel density have been unsuccessful (our unpublished observations) due to the extensive tumor necrosis resulting from our treatment. However, other mechanisms are possible, including the release of cytotoxic or inhibitory cytokines; elimination of stromal cells, such as the myeloid suppressor cells and regulatory T cells, in the milieu of the tumor neovascular network, which are known to express VEGFR-2 (57, 58); and/or interference with the incorporation of new endothelial cells into the vascular network. Further, the CAR-transduced cells selectively localized to the tumor vasculature rather than infiltrated into the tumor parenchyma at the times tested, as shown in Figure 7D. Although direct cross-presentation and priming of tumor-associated antigens was not checked directly, we did note that splenocytes of CAR-treated mice tested 30 days after treatment did develop low levels of reactivity against the B16-F10 tumor cells pulsed with gp100 peptide. This, however, could be due to the immunogenic effect of tumor eradication because of the CAR treatment.

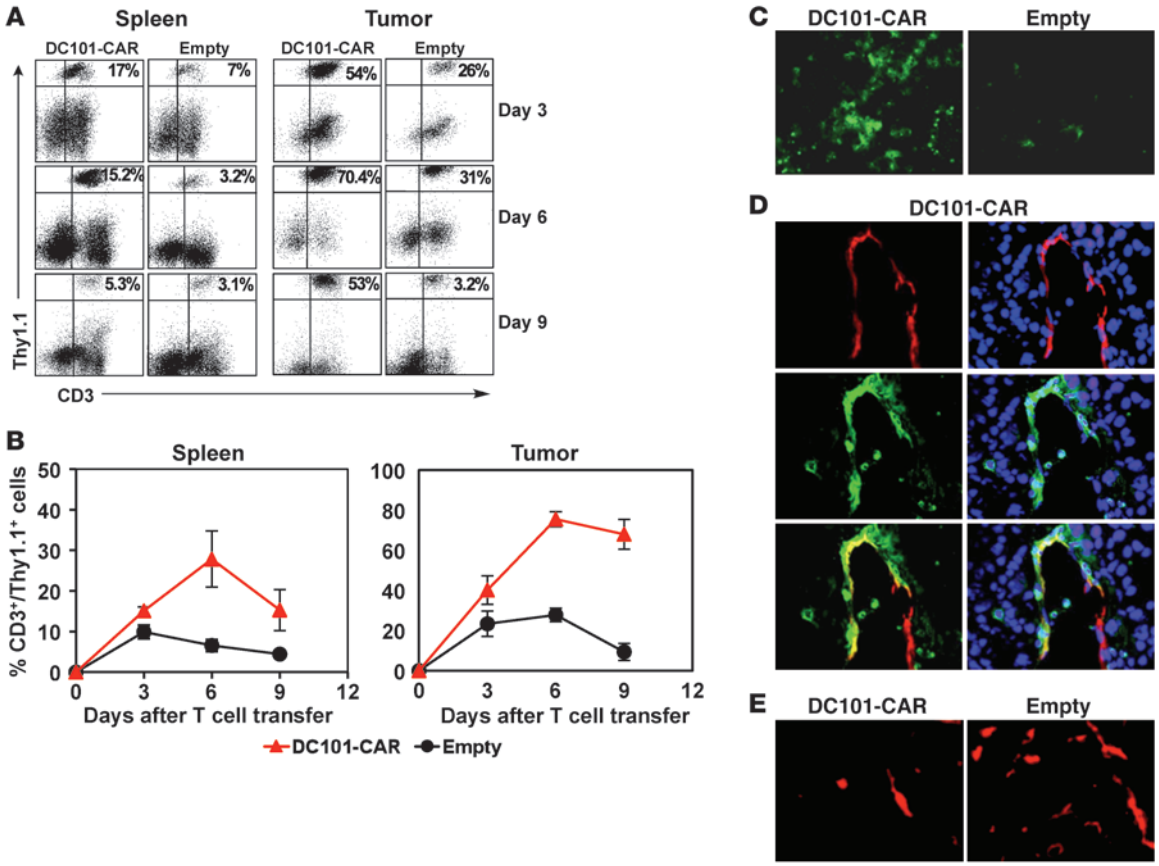

Figure 7

Enhanced tumor infiltration of adoptively transferred DC101-CAR–transduced T cells in mice bearing established B16-F10 tumor. C57BL/6 mice bearing B16-F10 tumor were treated with 2×10^7 DC101-CD828BBZ CAR- or empty vector–transduced Thy1.1$^+$ syngeneic T cells plus rhIL-2. Tumors and spleens from individual mice from each group were excised and processed to obtain single cell suspensions and analyzed by flow cytometry. (**A**) Representative FACS data from 3 experiments. (**B**) Pooled data obtained from 3 different mice from independent experiments (mean ± SEM). (**C**–**E**) Tumor samples were obtained from C57BL/6 mice bearing B16-F10 tumors treated with DC101-CD828BBZ CAR- or empty vector–transduced T cells and rhIL-2 on day 4 after ACT. Tumor sections were stained for Thy1.1 antigen expressed on transferred T cells (green) or the endothelial cell marker CD31 (red) together with DAPI (blue) to show the nucleus and analyzed using fluorescence microscopy. (**C**) Enhanced infiltration of adoptively transferred DC101-CD828BBZ CAR–transduced Thy1.1$^+$ T cells into tumor (original magnification, ×10). (**D**) Different area of the same tumor section (original magnification, ×40) from a mouse treated with DC101-CAR–transduced T cells presented in **C**, showing infused Thy1.1$^+$ T cells localized in and around the tumor vessels on day 4 after ACT. Yellow represents areas of colocalization of Thy1.1$^+$ T cell (green) and endothelial cells (red). (**E**) CD31 (red) staining of tumor vessels in a representative section, showing reduction in vessels in the tumor of a mouse treated with DC101-CD828BBZ CAR-transduced T cells at day 6 after ACT (original magnification, ×10).

The in vivo antitumor activity of DC101-CAR–transduced T cells was directly related to the number of cells administered and was similar when using constructs with or without the addition of the 4-1BB signaling chain, though the presence of this signaling sequence enhanced the persistence of the transferred cells at the tumor site. Similar to the results seen in extensive studies of ACT of the B16 melanoma using TCR transgenic T cells (59), the antitumor impact of the transferred VEGFR-2 CAR-transduced T cells was enhanced by the concomitant administration of IL-2. In contrast to the results reported using transgenic cells (39), lymphodepletion of the host prior to cell transfer did not appear to be essential for the therapeutic effect of the VEGFR-2 CAR.

Immune-mediated tumor eradication requires the adequate expansion, trafficking, and intra-tumoral activation of tumor antigen-specific T cells at the tumor site. In human clinical trials, in vivo persistence of adoptively transferred T cells was shown to be highly correlated with objective responses in patients treated with either tumor-reactive tumor infiltrating lymphocytes (60) or highly active TCR-engineered PBLs (36, 37). Suboptimal T cell activation can result in anergy and apoptosis, thereby aborting effective tumor immunity. To overcome these pitfalls, recent efforts have focused on the generation of CARs containing intracellular signaling sequences that provide additional costimulatory signaling in series with the TCR-ζ chain that could enhance the function of the CAR-modified T cells (61, 62). Most such extended CAR designs have used the signaling domains of CD28, a T cell costimulatory molecule with important functions in IL-2 production, proliferation, and cell survival of lymphocytes (63). The addition of CD28 signaling into CARs, along with the TCR-ζ chain, increased the expression of the CAR in transduced T cells, enhanced the proliferative capacity and IL-2 secretion of CAR-transduced T cells, and improved their in vivo antitumor effect (61, 62, 64–66).

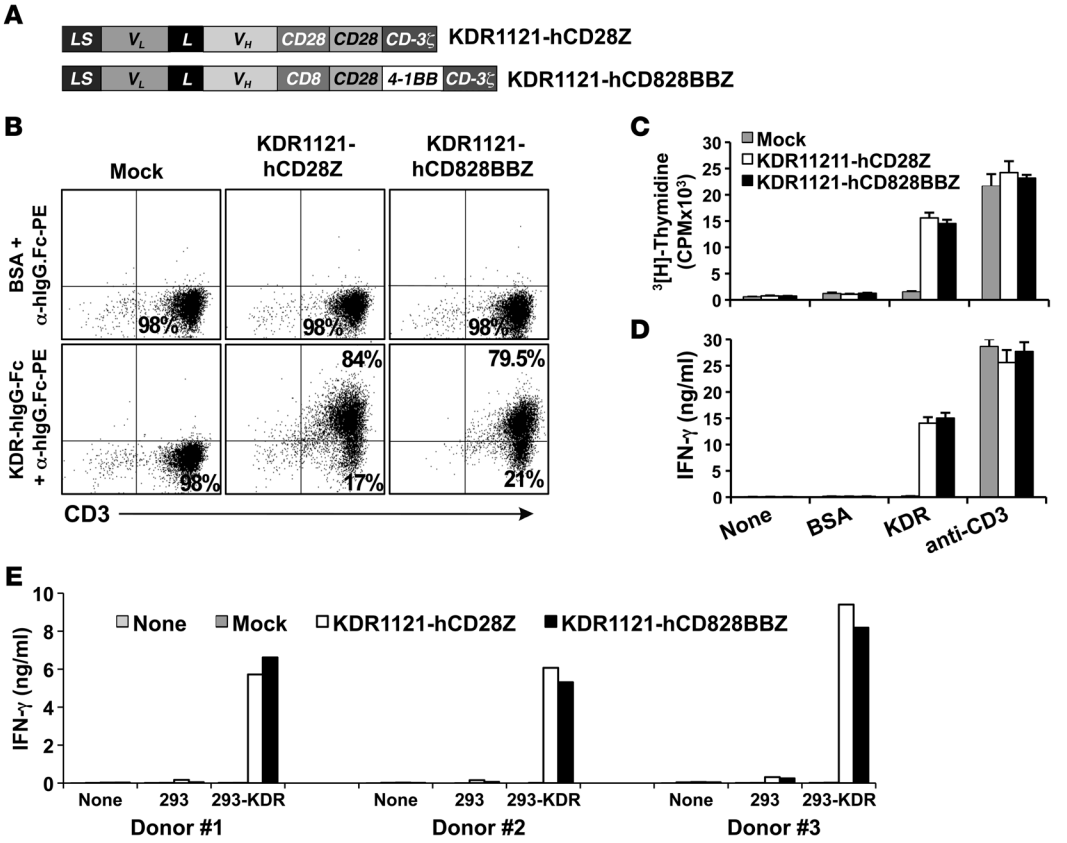

Figure 8

Construction and characterization of retroviral vectors encoding a CAR targeted against human VEGFR-2. (**A**) KDR1121, a ScFv comprising the V_L and V_H of fully human IgG specific to human KDR antigen, fused by a 218-linker sequence (*L*). CD28, 4-1BB, and CD3-ζ intracellular T cell signaling domains derived from human *CD28*, *TNFRSF9*, and *CD3* genes, respectively. *LS*, mouse immunoglobulin κ chain leader sequence; CD8, hinge and transmembrane regions from human CD8α. (**B**) Representative FACS data from 3 different donors transduced similarly with KDR1121-CD828Z or KDR1121-hCD28BBZ CAR-encoding retroviral vectors, showing the percentage of CD3$^+$ T cells expressing KDR-CAR in the top right quadrants and the percentage of CD3$^+$ T cells negative for KDR-CAR expression in the bottom right quadrants. (**C** and **D**) Primary human T cells were transduced with the indicated retroviral vectors. Seven days later, cells were cultured on antigen-coated 96-well microtiter plates for 3 days. (**C**) Cell proliferation was measured as [^{3}H]thymidine incorporation during the last 16 hours. (**D**) Culture supernatants were assayed for IFN-γ by ELISA. Results are presented as the mean ± SEM of triplicates. (**E**) Primary human T cells from 3 different donors were mock transduced or transduced with KDR1121-hCD828BBZ CAR-expressing retroviral vector and, 8 days later, cocultured with the indicated cell lines for 24 hours. Culture supernatants were assayed for IFN-γ by ELISA.

Recently several studies have explored the use in CAR of intracellular signaling sequences of 4-1BB, a costimulatory molecule known to promote differentiation and enhance long-term survival as well as cytolytic function of CD8 T cells (67–70), in addition to the CD28 and CD3-ζ signaling sequences. In multiple studies these CAR-transduced T cells were protected from activation-induced cell death and showed enhanced survival, expansion, and cytokine secretion and as well as consistently demonstrating long-term persistence and antitumor effects in vivo when targeting tumor-associated antigens in tumor-bearing mice (61, 66, 71–73). In the studies reported here, we documented an increased persistence of T cells transduced with 4-1BB containing DC101-CAR in the tumor compared with cells transduced with a vector lacking 4-1BB. However, their in vivo antitumor effects were comparable.

Most effective tumor immune strategies require both fully armed effector cells and a tumor microenvironment permissive for infiltration of T cells into the tumor. One of the major advantages of the VEGFR-2 CAR approach is the ability to mediate tumor destruction independent of the ability of T cells to extravasate into the tumor site, since the target molecules are present on the surface of the tumor vasculature. Our immunohistochemical studies suggest that the CAR-transduced T cells colocalize to the tumor endothelial cells. Several studies have demonstrated that treatment of tumor-bearing mice with angiogenesis inhibitors can enhance lymphocyte trafficking and infiltration into the tumor (53, 74). The VEGFR-2 CAR-engineered T cells exhibited increased infiltration into the tumor compared with the empty vector-transduced T cells, suggesting that endothelial cell destruction renders the tumor vessels more permissive for extravasation and infiltration of adoptively transferred T cells into the tumor. As some human tumor cells have been reported to express VEGFR-2 on their surface (3, 9, 75), this may enhance antitumor effects when this approach is translated to the treatment of patients with cancer.

A primary concern of targeting angiogenic receptors is interference with normal angiogenesis or recognition of the low levels of VEGFR-2 on normal vessels (41, 42, 44). Previous studies reported that active immunization against VEGFR-2 exhibited no

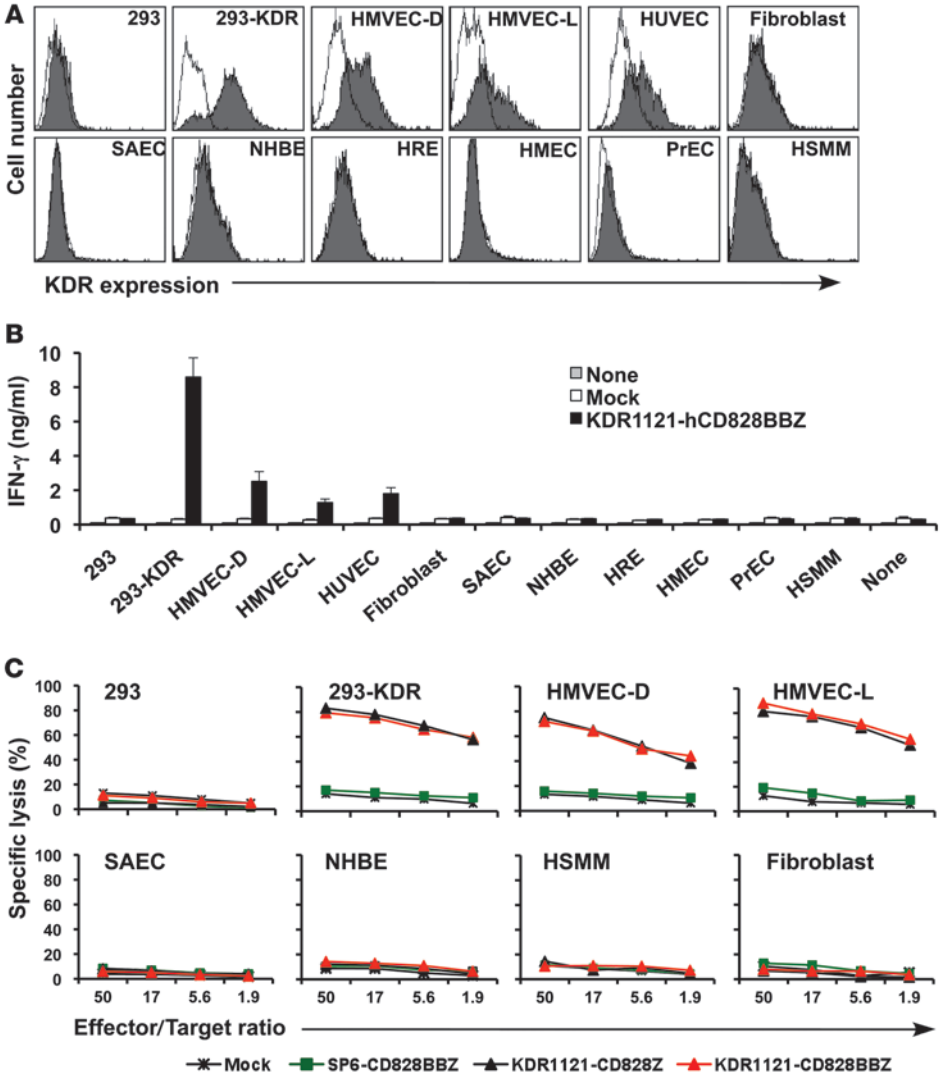

Figure 9
Recognition of KDR-expressing primary human cells by KDR-CAR–transduced PBLs. (**A**) KDR expression on various normal primary human cells. The indicated human cell types were stained with PE-labeled mouse anti-human KDR antibody or isotype control antibody and analyzed by FACS. The filled histograms indicate KDR-specific staining; the open histograms indicate staining with isotype control antibody. (**B**) Primary human T cells were mock transduced or retrovirally engineered to express KDR1121-hCD828BBZ CAR and, 8 days later, cocultured with indicated human cells for 24 hours. Culture supernatants were assayed for IFN-γ by ELISA. Results are presented as mean ± SEM of triplicates. (**C**) The cytotoxicity of genetically engineered primary human T cells expressing KDR1121-hCD828BBZ or KDR1121-hCD28Z CAR against indicated target cells was determined by using a standard Cr^{51} release assay. Each data point reflects the mean of triplicates.

toxicity (20–25, 54), although caution should be taken in interpreting these reports, since vaccine induced CTLs may be of low avidity due to immunological self-tolerance. The toxicity associated with the administration of large numbers of VEGFR-2 CAR-expressing T cells in BALB/c mice but not in C57BL/6 mice is under study and may be related to the known polarization of BALB/c mice to a Th2 phenotype compared with C57BL/6 mice (76, 77).

Recently performed pilot clinical studies in patients with metastatic cancer have used CAR-modified T cells targeting tumor antigens (78–82). While most of these studies failed to induce any measurable antitumor effect, the safety of this approach was established (78, 81, 82). However, in one study, patients treated with adoptive transfer of autologous T cells modified with CARs against carbonic anhydrase IX exhibited biliary toxicity due to recognition of this determinant on epithelial cells lining bile ducts (79, 80). In a clinical study, individuals with neuroblastoma were treated with genetically engineered Epstein-Barr virus–specific cytotoxic lymphocytes expressing a CAR directed to the disialoganglioside GD2, a nonviral tumor–associated antigen expressed by human neuroblastoma cells, which resulted in tumor regression in a minority of the subjects treated without any reported toxicity (38).

To translate our findings in the mouse to the treatment of human cancers, we generated recombinant retroviral vectors encoding CARs composed of a fully human ScFv targeted against the human VEGFR-2 antigen and demonstrated their ability to generate target-specific immune responses in vitro. The VEGFR-2 CAR-transduced human T cells did not recognize normal primary human epithelial cells in in vitro assays. Taken together, this preclinical study provides a rationale for the translation of VEGFR-2 CAR-transduced cells for the treatment of human cancer, and we are currently generating a good manufacturing practice–quality retrovirus encoding anti-human VEGFR-2 for use in these studies.

Methods

Mice. Inbred female C57BL/6 mice were purchased from the National Cancer Institute–Frederick Cancer Research and Development Center (NCI-Frederick). BALB/c mice were purchased from The Jackson Laboratory. All animal studies were performed in accordance with the Animal Care and Use Committee guidelines of the NIH and were conducted under protocols approved by the Animal Care and Use Committee of the NCI.

Cell culture. The murine tumor lines used in this study were B16-F10 (melanoma), MCA-205 (sarcoma), MC38 (colon adenocarcinoma), MB49

(bladder carcinoma), MC17-51 (sarcoma), CT26 (colon carcinoma), RENCA (renal carcinoma), 4T1 (mammary adenocarcinoma), C-1498 (myeloid leukemia), EL-4 (lymphoma), and NIH-3T3 (mouse embryonic fibroblast). B16-F10, MCA205, MC38, and NIH-3T3 cells were obtained from the cell culture depository of the Surgery Branch, NCI. CT26 and RENCA cells were obtained from Jonathan Weiss (NCI-Frederick). SVEC4-10EHR1, MS1, and SVR transformed mouse endothelial cell lines were purchased from ATCC. eBEND.3 is also a transformed mouse endothelial cell line (provided by Frank Cuttita, Angiogenesis Core Facility, NCI, Gaithersburg, Maryland, USA). MB49-Flk1 and NIH3T3-Flk1 cells stably expressing mouse VEGFR-2 protein were generated in our laboratory by transducing the MB49 and NIH-3T3 cell lines with a VSV-G pseudotyped lentiviral vector encoding full-length mouse VEGFR-2 (ref. 44 [provided by Lena Claesson-Welsh, Uppsala University, Uppsala, Sweden]).

PBLs used in this study were cryopreserved PBMCs obtained by leukapheresis of the blood of metastatic melanoma patients treated at the Surgery Branch, NCI. Any patient-derived material used in this study was received after obtaining informed consent and was approved by the Institutional Review Board of NCI. The following normal primary human cells used in this study were procured from Lonza Walkersville Inc.: HMVECs, HMVEC-L, HMVEC-D, HUVECs, small airway epithelial cells (SAEC), bronchial/tracheal epithelial cells (NHBE), renal epithelial cells (HRE), mammary epithelial cells (HMECs), prostate epithelial cell (PrECs), smooth muscle myoblasts (HSMM), and skin fibroblasts. Other cell lines used were human embryonic kidney fibroblast cell lines 293 and 293-KDR, a stable transfectant expressing KDR (provided by Maria Parkhurst, Surgery Branch, NCI). The retroviral packaging cell lines 293GP and PG13 were obtained from ATCC. The ecotropic packaging cell line Phoenix Eco cells was provided by Gary Nolan (Stanford University, Stanford, California, USA).

All the mouse tumor lines described above were maintained in R10 (RPMI 1640 medium supplemented with 10% heat-inactivated FBS, 100 U/ml penicillin, and 100 μg/ml streptomycin; all from Invitrogen Corp.). All the mouse endothelial cell lines (NIH-3T3, 293, 293-KDR, 293GP, PG13, and Phoenix Eco cells) were maintained in D10 (DMEM [Invitrogen Corp.] supplemented with 10% heat-inactivated FBS, 100 U/ml penicillin, and 100 μg/ml streptomycin). All the primary human cells were maintained in their respective culture media purchased from Lonza Walkersville Inc. Mouse T cells were cultured in RPMI 1640 containing 10% heat-inactivated FBS, 100 U/ml penicillin, 100 μg/ml streptomycin, 0.05 mM 2-mercaptoethanol, 0.1 mM MEM non-essential amino acids, 1 mM pyruvate, and 2 nM L-glutamine (all from Invitrogen Corp) and 30 IU/ml of rhIL-2 (Chiron). Primary human lymphocytes were cultured in culture medium containing 50% RPMI 1640, 50% AIM-V medium, and 0.05 mM mercaptoethanol (all from Invitrogen Corp.), 10% heat-inactivated human AB serum (Gemini Bio-Products), and 300 IU/ml rhIL-2. All the cells were cultured at 37°C under 5% CO_2 and 95% humidity.

Construction of MSGV retroviral vectors encoding CARs. The CAR constructs used in this study are schematically illustrated in Figure 1A and Figure 6A, and the order of placement of various signaling domains in different CAR constructs is described in the corresponding figure legends. The DC101-CD828BBZ CAR comprising a ScFv against mouse VEGFR-2, referred as DC101 ScFv, derived from DC101 antibody, a rat anti-mouse IgG against mouse VEGFR-2 (Imclone Systems Inc.) linked in-frame to the hinge and transmembrane regions of the mouse CD8α chain (nucleotide sequence 580–795 corresponds to Genbank NM 001081110), which in turn fused to the mouse intracellular signaling sequences derived from mouse CD28 (nucleotide sequence 618–740 corresponds to Genbank NM 007642), 4-1BB (nucleotide sequence 779–913 corresponds to Genbank J04492), and CD3-ζ (nucleotide sequence 313–635 corresponds to Genbank NM 001113391) molecules. The DC101-CD828Z construct has the same components in similar configuration and order, except that it lacked the 4-1BB signaling domain. In the DC101-CD8 construct, only the DC101 ScFv and the hinge and transmembrane sequences of mouse CD8α were included. The SP6-CD828BBZ (SP6-CAR) construct is similar to that of DC101-CD828BBZ CAR, except that the DC101 ScFv was replaced with a SP6 ScFv. It recognizes a hapten 2, 4, 6-trinitrophenyl (TNP). MSGV vector encoding the SP6-CAR or an empty MSGV vector not carrying a transgene were used as control vectors in this study.

A full-length 806-bp DC101 ScFv was constructed using the polymerase chain amplification and assembly technique as follows. The coding sequences for variable regions of heavy (V_H) and light chains (V_L) were amplified separately and recombined using a linker by subsequent PCR reaction. The first set of PCR reactions were performed to amplify the leader sequence (*LS*) and the V_H and also the V_L. The plasmids DC101 HC (clone 8.6) pCR2.1-TOPO and DC101 LC (clone 3.2) pCR2.1-TOPO, containing the heavy and light chain coding sequences, respectively, of the DC101 antibody (provided by Dale Ludwig, Imclone Systems Inc.), were used as templates in the first PCR reactions to generate the *LS* plus V_H and V_L components of DC101 ScFv. The heavy chain forward primer (heavy forward, 5′-TCGCTCGAGGCCGCCACCATGGGATGGTCAT-3′) was designed to span through the 5′ end of the heavy chain *LS* and contains an *XhoI* site at its 5′ end (underlined text). The light chain reverse primer (V_L reverse, 5′-TCGGCGGCCGCTTTCAGTTCCAGCTTGGTCCCAGC-3′) contains a *Not*I site (underlined text) at its 3′ end. The light chain forward primer (V_L forward, 5′-CTGGGAAGCCGGGTTCTGGTGAGGGTTCTGA-CATTGTGCTGACCCAGTCTCCT-3′) was designed to include part of the 218-linker sequence and is compatible with the heavy chain reverse primer (V_H reverse, 5′-ACCAGAACCCGGCTTCCCAGATCCAGATGTAGACCCT-GAGGAGACTGTGACCATGACTCC-3′). In the second PCR reaction, the first PCR products — the heavy chain *LS* plus V_H and V_L fragments — were assembled and amplified using the heavy forward and V_L reverse primer set, which resulted in the final DC101 ScFv fragment. The synthesized DC101 ScFv DNA fragments were sequence confirmed.

The nucleotide sequences of mouse CD8α hinge and transmembrane regions and the intracellular signaling domains of mouse CD28, 4-1BB, and CD3-ζ described earlier were assembled in-frame in order to produce 2 different configurations referred to as CD828BBZ or CD828Z. Both of these fragments were designed to have a *Not I* site at 5′ end and the *SalI* and *BamH1* sites at 3′ end and were synthesized by GeneArt AG. The plasmids encoding these sequences were digested with *NotI* and *BamHI* restriction enzymes (New England Biolabs) and ligated individually into the similarly digested MSGV vector plasmid described previously (66). This subcloning step created 2 interim retroviral constructs, namely MSGV-4D5-CD828BBZ and MSGV-4D5-CD828Z. To generate the DC101-CAR–encoding retroviral vectors MSGV-DC101-CD828BBZ (referred to as DC101-CD828BBZ) and MSGV-DC101-CD828Z (referred to as DC101-CD828Z), the *XhoI*- and *NotI*-digested DC101 ScFv fragment was directly ligated into the MSGV-4D5-CD828BBZ and MSGV-4D5-CD828Z plasmids, replacing the 4D5 fragment.

To generate a MSGV-DC101-CD8 (referred to as DC101-CD8), the DC101-CD8 nucleotide sequence was amplified from the MSGV-DC101-CD828Z plasmid by PCR reaction, using the primer set heavy forward and a reverse primer ACGGTCGACTTATCGGCTCCTGTGGTAGCAGATGA, which contains a TAA stop codon, followed by a SalI restriction site (underlined text). The PCR product was digested with *XhoI* and *SalI* and ligated into a similarly digested MSGV-DC101-CD828Z plasmid, replacing the DC101CD828Z fragment. The MSGV-SP6CD828BBZ CAR (referred to as SP6-CD828BBZ or SP6-CAR) was created as follows. The SP6 ScFv fragment was PCR amplified from a plasmid encoding the SP6-ScFv (83), using the primers SP6 forward, 5′-TCGCTCGAGCTCTAGACCGC-CATGGATTTTCAG-3′, which contains a *XhoI* site (underlined text), and

SP6 reverse, 5′TCGGCGGCCGCGGTGACCGTAGTTCCTTGGCCC-3′, which contains a *NotI* site (underlined text). A plasmid encoding the SP6 ScFv was provided by Z. Eshhar (Weizmann Institute of Science, Rehovot, Israel). The PCR product was then digested with *XhoI* and *NotI* enzymes and cloned into the similarly digested MSGV-DC101-CD828BBZ plasmid replacing the DC101 ScFv.

The human VEGFR-2–specific (KDR-specific) ScFv was derived from KDR-1121 antibody, a fully human IgG against human KDR protein, referred to as KDR1121-ScFv. The amino acid sequences of KDR-1121 V_L and V_H were derived from a published report (45). The KDR ScFv containing the mouse immunoglobulin κ chain *LS*, followed by the codon optimized V_L and V_H sequences derived from KDR-1121 antibody, linked by the 218 linker, was designed and synthesized using a web-based DNA codon optimization algorithm (84), using the primers generated by UpGene (http://www.vectorcore.pitt.edu/upgene/upgene.html) (Supplemental Figure 5). The synthesized KDR1121 ScFv DNA fragments were sequence confirmed and subcloned in-frame into the MSGV retroviral vector containing the human CD28 hinge and transmembrane sequences linked to the human CD28 and CD3-ζ intracellular signaling moieties described previously (65) to generate the MSGV-KDR1121-CD28Z vector. To obtain the MSGV-KDR1121-CD28BBZ vector, the KDR1121 ScFv was cloned in-frame into a similar MSGV vector (66), containing the hinge and transmembrane sequences of human CD8α chain linked to the cytoplasmic signaling domains of human CD28, 4-1BB, and CD3-ζ molecules, using the standard molecular biology techniques. The sequence integrity of all the vectors described in this paper was confirmed by DNA sequencing. All the molecular constructs were cloned into a retroviral vector (MSGV) containing a murine stem cell virus long-terminal repeat (known to be relatively resistant to in vivo silencing), incorporating the splicing and optimized the start codon of the MFG design of vectors described previously (85).

Retrovirus production. Retroviral vector supernatant was produced from stable packaging cell lines or by transient transfection. To generate stable packaging cell lines for retroviral vectors encoding MSGV-DC101-CD828BB or MSGV-DC101-CD828Z, 9 μg of the plasmid DNA of each of these retroviral vector plasmid DNAs were transfected individually into PG13 cells, using the Lipofectamine 2000 transfection reagent (Invitrogen Corp.). Supernatant from these transfected cells was harvested 48 hours later and used to transduce Phoenix Eco cells in the presence of 8 μg/ml protamine sulfate (Sigma-Aldrich). The transduction was repeated the next day, and 16 hours later, transduced Phoenix Eco cells were subjected to limiting dilution cloning. Clones were expanded and high-titer clones were selected by the dot-blot titration method, as described previously (86). Retroviral supernatants from these stable producer clones were used to transduce mouse T cells in subsequent experiments. Retroviruses encoding the empty vector, DC101-CD8, or SP6-CAR, described in this study, were produced transiently. To generate transient viral supernatant, 293GP cells were cotransfected with retroviral vector plasmid and an ecotropic envelope encoding plasmid (Clontech) using Lipofectamine 2000 reagent (Invitrogen Corp.). Supernatants containing the retrovirus were collected 48 hours later and used to transduce mouse T cells. PG13-based stable high-titer packaging cell clones for retroviral vectors encoding MSGV-KDR1121-CD828BBZ and MSGV-KDR1121-CD828Z were generated, as described previously (87), and supernatants from these stable producer clones were used to transduce human T cells.

Retroviral transduction of mouse and human T cells. To obtain mouse T lymphocytes, spleens obtained from 8- to 10-week-old mice were crushed through a 40-μm cell strainer (BD Biosciences) and subjected to red blood cell lysis. $CD3^+$ T cells were purified by using the Dynal Mouse T cell Negative Isolation Kit (Invitrogen Corp.). Mouse T cells were stimulated for 24 hours in culture media in the presence of 30 IU/ml rhIL-2, 2 μg/ml ConA (Sigma-Aldrich), and 1 ng/ml recombinant mouse IL-7 (R&D Systems) prior to transduction and thereafter maintained in the culture media containing 30 IU/ml rhIL-2 alone. (83). In some experiments, $CD8^+$ and $CD4^+$ mouse T cells were purified using Dynal-negative $CD8^+$ or $CD4^+$ T cell enrichment kit prior to transductions with retroviral vectors. The human PBLs were cultured as described previously (87). Both the mouse and human lymphocytes were transduced with retroviral vectors, using a similar transduction protocol as that described previously (83).

Detection of CAR expression on transduced T cells. Expression of DC101-CAR and KDR-CAR on retrovirally transduced mouse and human T cells, respectively, was detected by indirect immunofluorescence with soluble mouse or human VEGFR-2–hIgG.Fc fusion protein (R&D Systems), followed by staining with a PE-labeled goat anti-human IgG.Fc (α-hIgG.Fc) antibody (eBioscience). Expression of SP6-CAR on transduced $CD8^+$ mouse T cells was detected as described previously (87). Mouse and human T cells were costained with allophycocyanin-labeled (APC-labeled) anti-mouse CD8 or anti-human CD3 antibodies (both from BD Pharmingen), respectively. Aliquots of cells stained with BSA (Sigma-Aldrich) and PE-labeled α-hIgG.Fc antibody served as controls to determine the specificity of CAR staining and the MFI of its expression on transduced T cells by FACS. For analysis, the relative log fluorescence of live cells was determined using a FACSCalibur flow cytometer, equipped with CellQuest software (BD Biosciences).

Generation of mouse cell lines stably expressing mouse VEGFR-2. The lentiviral vector expressing the full-length coding region of mouse VEGFR-2 fused to the EGFP, referred to as pFUGIE-Flk1, was a gift from Lena Claesson-Welsh (Uppsala University). MB49 and NIH-3T3 mouse cell lines were transduced with a vesicular stomatitis virus G protein–pseudotyped pFUGIE-Flk1 vector at a multiplicity of infection of 10 in the presence of 10 μg/ml protamine sulfate. After 2 passages, the EGFP-positive cells were sorted by FACS, using a FACSVantage SE machine with FACSDiva software (BD Biosciences).

Detection of VEGFR-2 expression on mouse and human cells. Detection of cell surface expression of endogenous or transgenically expressed VEGFR-2 protein on various mouse cell lines was achieved by using 3-step indirect immunofluorescence staining protocol. Briefly, cells were harvested (adherent cells were harvested using a cell scraper [Corning Incorporated] and washed in FACS buffer [PBS containing 1% FBS]) and resuspended in FACS buffer. Aliquots of 5×10^5 cells were incubated with 1 μg recombinant DC101 antibody for 45 minutes at 4°C. Cells were then washed twice in FACS buffer and successively incubated with 1 μg soluble mVEGFR-2–hIgG.Fc protein and PE-labeled goat anti-human IgG.Fc antibody each for 30 minutes at 4°C. Cells were then washed and analyzed by flow cytometry. Cells stained similarly, but with rat IgG1 isotype control antibody instead of DC101 antibody in the first incubation step of the protocol, served as control. VEGFR-2 expression on various mouse cell lines was also determined by FACS using the PE-labeled rat anti-mouse antibody against the mouse VEGFR-2 (BD Biosciences), following the manufacture's instructions. Expression of VEGFR-2 (KDR) on human 293, 293-KDR, and various primary human cells was determined by staining them with PE-labeled mouse anti-human VEGFR-2 antibody (R&D Systems), following the manufacturer's instructions. Cells stained with PE-labeled mouse IgG_1 (R&D Systems) were used as controls to determine the specificity of KDR staining. Flow cytometry acquisition was performed with a FACS Calibur flow cytometer (BD Biosciences). Data were acquired and analyzed using CellQuest software (BD Biosciences). A combination of forward angle light scatter and propidium iodide staining was used to gate out dead cells. The specificity of VEGFR-2 staining and the MFI of its expression on various cell types was determined using respective cell types stained with PE-conjugated isotype control antibody.

FACS analysis of various cell surface markers and chemokine receptors on mouse T cells. Enriched splenic $CD3^+$ T cells were transduced with the various retroviral vectors. Five days after transduction, cells were costained with APC-conjugated hamster anti-mouse CD3 antibody (BD Biosciences) and

one of the following antibodies labeled with PE: rat anti-mouse CD62L (BD Biosciences), rat anti-CCR7 (BD Biosciences), mouse anti-mouse CCR9 (eBioscience), hamster anti-mouse CXCR3 (eBioscience), and rat anti-mouse CXCR4 (BD biosciences). Cells were stained with the indicated antibodies, as recommended by the manufacturers, and analyzed by FACS. Aliquots of cells stained with relevant fluorochrome-labeled species and isotype-specific control antibodies were used to determine the specificity of staining and the MFI of its expression. For analysis, the relative log fluorescence of live cells was determined using a FACS Calibur flow cytometer equipped with CellQuest software (BD Biosciences).

Proliferation, IFN-γ release, and cytotoxicity assays. Transduced mouse or human T cells were tested for specific reactivity against plate-bound VEGFR-2 protein as well as target cells expressing VEGFR-2 in proliferation and IFN-γ release assays. Untreated microtiter plates were coated individually with 5 μg/ml BSA, 5 μg/ml soluble mouse or human VEGFR-2–hIgG.Fc fusion protein, 2 μg/ml of a purified anti-mouse CD3 antibody (clone 145-2C11, BD Pharmingen), or 2 μg/ml OKT3 (Orthoclone) diluted in PBS for 3 hours at 37°C. Mouse T cells and human PBLs, 4 or 8 days after transduction, respectively, were plated at 10^5 cells per well on antigen-coated microtiter plates or cocultured with species-specific target cells in 200 μl culture volume. Cell proliferation was determined after 3 days of culture by tritiated thymidine incorporation assay. Culture supernatants harvested at 24 to 48 hours after culture were assayed for IFN-γ using commercially available ELISA kits (Pierce-Endogen). The cytotoxicity of T cells against tumor target cells was measured using a ^{51}Cr release assay (66). Maximal release was calculated after incubating target cells in 1% Triton X-100. In some experiments, target cells were incubated with 10 μg/ml of the rat IgG1, DC101 (rat anti-mouse VEGFR-2), or the goat anti-mouse VEGFR-1 (R&D Systems) antibodies at 37°C for 1 hour prior to coculture with the effector T cells. Supernatants were harvested 24 hours later and assessed for IFN-γ by ELISA. The assays were performed in triplicate wells and values are represented as mean ± SEM.

Tumor models and adoptive transfer. At 6 to 7 weeks of age, mice were injected subcutaneously with 5×10^5 syngeneic tumor cells, and 10–12 days later, mice were treated with i.v. adoptive transfer of 2×10^7 or indicated numbers of syngeneic $CD3^+$ mouse T cells transduced with various retroviral vectors. Starting volumes of tumors ranged from 30 to 80 mm^2. Unless indicated otherwise, lymphopenia was induced by nonmyeloablative (5 Gy) TBI of mice on the day of adoptive transfer. Cell transfer in mice occurred concomitantly with i.p. injection of rhIL-2 (100,000 CU/dose/mouse), twice a day, with at least a 6- to 8-hour interval, for 3 days. If indicated, B16-F10 tumor-bearing mice were injected i.p. with a single dose of recombinant DC101 antibody or rat IgG_1, both at 800 μg/dose/mouse in 500 μl PBS (Invitrogen Corp.). All experiments were performed independently, at least twice with similar results, in a double-blinded, randomized fashion. Each treatment group included a minimum of 5 mice. Serial, blinded tumor measurements were obtained, and the products of perpendicular diameters were plotted ± SEM. Statistics on tumor growth inhibition were calculated using the Wilcoxon rank-sum test, based on linear slopes of the tumor growth curves at each data point. *P* values of 0.05 or lower were considered significant.

Evaluation of in vivo persistence of adoptively transferred T cells. Spleens and tumors from 3 mice in treatment groups were harvested at the indicated time points, and single cell suspensions were made by crushing the tissues through a 40-μm cell strainer. Splenocytes were obtained after red cell lysis, and lymphocytes were further separated from the tumor cell suspensions by density gradient centrifugation using Lympholyte-M (Cedarlane Laboratories). The phenotype of cell preparations was determined by direct staining of cells with APC-conjugated rat anti-mouse CD3 and PE-labeled mouse anti-rat Thy1.1 antibody (both from BD Pharmingen). Aliquots of cells were stained with relevant isotype control antibodies to determine the specificity of staining. The percentage of viable $CD3^+Thy1.1^+$cells in the lymphocyte-gated population of the tumor cell preparations and all the viable cell populations of splenocytes was determined by FACS.

Immunofluorescent microscopy. For immunofluorescence study, B16-F10 tumors were excised and embedded in OCT media (Tissue-Tek). Cryostat sections (8 to 10 μm) were prepared on silanated glass slides, fixed in cold acetone for 10 minutes, blocked with 2.5% normal goat serum (Jackson ImmunoResearch Laboratories Inc.) for 30 minutes, and incubated overnight at 4°C with the following primary antibodies: purified rat anti-mouse CD31 or isotype (MEC 13.3 and R35-95; BD Biosciences), biotinylated mouse anti-Thy1.1 or isotype (OX-7 and MOPC-31C; BD Biosciences), or combinations of anti-CD31 and anti-thy1.1 or isotype controls. Secondary immunofluorescent labeling of the Thy1.1 and CD31 antigens was performed with Fluorescein-conjugated (DTAF-conjugated) streptavidin for 30 minutes or Cy-5–conjugated goat anti-rat IgG $F(ab')_2$ (Jackson ImmunoResearch Laboratories Inc.) for 60 minutes at room temperature. For CD31 and Thy1.1 dual labeling, streptavidin-DTAF incubation was performed first, followed by Cy-5–conjugated goat anti-rat incubation. To determine the coexpression of CD31 and VEGFR-2 on tumor vessels, B16-F10 tumor sections were costained with FITC-labeled rat anti-mouse CD31 antibody (MEC 13.3, BD) and PE-labeled rat anti-mouse VEGFR-2 (AVAS 12α1) or respective fluorochrome-conjugated isotype control antibody rat IgG2a, k (all from BD Biosciences) for 30 minutes. Slides were mounted with DAPI containing mounting media (Prolong Gold, antifade reagent with DAPI; Invitrogen Corp.). Tumor sections were evaluated for $Thy1.1^+$ lymphocytic infiltration, CD31, and VEGFR-2 expression on vessels by using an Olympus IX51/IX71 epifluorescence inverted microscope (Olympus), and the images were digitally captured using an Olympus IRDP71 digital camera and analyzed using DP-BSW software (Olympus).

Statistics. The statistical significance of tumor growth inhibition between the experimental groups was calculated using the Wilcoxon rank-sum test, based on linear slopes of the tumor growth curves at each data point. *P* values of 0.05 or lower were considered significant.

Acknowledgments

We thank Douglas Palmer, Lindsay Church, Robert Reger, Dorina Frasheri, and David Jones (Surgery Branch, NCI) for helping us with the animal studies. We also thank Hui Xu (Surgery Branch, NCI) for help in preparing the retroviral producer cells and Arnold Mixon and Shawn Farid of the Flow Cytometry Unit (Surgery Branch, NCI) for help with flow cytometry.

Received for publication April 27, 2010, and accepted in revised form August 24, 2010.

Address correspondence to: Steven A. Rosenberg, Surgery Branch, National Cancer Institute, Clinical Research Center, Building 10-CRC, Room 3-3940, 10 Center Drive, MSC 1201, Bethesda, Maryland 20892, USA. Phone: 301.496.4164; Fax: 301.402.1738; E-mail: SAR@mail.nih.gov.

1. Carmeliet P. Mechanisms of angiogenesis and arteriogenesis. *Nat Med*. 2000;6(4):389–395.
2. Folkman J. Angiogenesis: an organizing principle for drug discovery? *Nat Rev Drug Discov*. 2007; 6(4):273–286.
3. Padro T, et al. Overexpression of vascular endothelial growth factor (VEGF) and its cellular receptor KDR (VEGFR-2) in the bone marrow of patients with acute myeloid leukemia. *Leukemia*. 2002; 16(7):1302–1310.
4. Folkman J, Watson K, Ingber D, Hanahan D. Induction of angiogenesis during the transition from hyperplasia to neoplasia. *Nature*. 1989;339(6219):58–61.
5. Hanahan D, Folkman J. Patterns and emerging mechanisms of the angiogenic switch during tumorigenesis. *Cell*. 1996;86(3):353–364.
6. Ferrara N, Alitalo K. Clinical applications of angiogenic growth factors and their inhibitors. *Nat Med*. 1999;5(12):1359–1364.
7. Brooks PC, et al. Integrin alpha v beta 3 antago-

nists promote tumor regression by inducing apoptosis of angiogenic blood vessels. *Cell*. 1994; 79(7):1157–1164.
8. Ferrara N, Gerber HP, LeCouter J. The biology of VEGF and its receptors. *Nat Med*. 2003;9(6):669–676.
9. Masood R, Cai J, Zheng T, Smith DL, Hinton DR, Gill PS. Vascular endothelial growth factor (VEGF) is an autocrine growth factor for VEGF receptor-positive human tumors. *Blood*. 2001;98(6):1904–1913.
10. Bergers G, Hanahan D. Modes of resistance to anti-angiogenic therapy. *Nat Rev Cancer*. 2008; 8(8):592–603.
11. Ebos JM, Lee CR, Cruz-Munoz W, Bjarnason GA, Christensen JG, Kerbel RS. Accelerated metastasis after short-term treatment with a potent inhibitor of tumor angiogenesis. *Cancer Cell*. 2009; 15(3):232–239.
12. Gupta K, Zhang J. Angiogenesis: a curse or cure? *Postgrad Med J*. 2005;81(954):236–242.
13. Paez-Ribes M, et al. Antiangiogenic therapy elicits malignant progression of tumors to increased local invasion and distant metastasis. *Cancer Cell*. 2009;15(3):220–231.
14. Witte L, et al. Monoclonal antibodies targeting the VEGF receptor-2 (Flk1/KDR) as an anti-angiogenic therapeutic strategy. *Cancer Metastasis Rev*. 1998;17(2):155–161.
15. Zhu Z, et al. Inhibition of vascular endothelial growth factor-induced receptor activation with anti-kinase insert domain-containing receptor single-chain antibodies from a phage display library. *Cancer Res*. 1998;58(15):3209–3214.
16. Prewett M, et al. Antivascular endothelial growth factor receptor (fetal liver kinase 1) monoclonal antibody inhibits tumor angiogenesis and growth of several mouse and human tumors. *Cancer Res*. 1999;59(20):5209–5218.
17. Rakhmilevich AL, Hooper AT, Hicklin DJ, Sondel PM. Treatment of experimental breast cancer using interleukin-12 gene therapy combined with anti-vascular endothelial growth factor receptor-2 antibody. *Mol Cancer Ther*. 2004;3(8):969–976.
18. Wang ES, Teruya-Feldstein J, Wu Y, Zhu Z, Hicklin DJ, Moore MA. Targeting autocrine and paracrine VEGF receptor pathways inhibits human lymphoma xenografts in vivo. *Blood*. 2004;104(9):2893–2902.
19. Yu JL, Rak JW, Coomber BL, Hicklin DJ, Kerbel RS. Effect of p53 status on tumor response to antiangiogenic therapy. *Science*. 2002;295(5559):1526–1528.
20. Wei YQ, et al. Immunotherapy of tumors with xenogeneic endothelial cells as a vaccine. *Nat Med*. 2000;6(10):1160–1166.
21. Li Y, et al. Active immunization against the vascular endothelial growth factor receptor flk1 inhibits tumor angiogenesis and metastasis. *J Exp Med*. 2002;195(12):1575–1584.
22. Niethammer AG, et al. A DNA vaccine against VEGF receptor 2 prevents effective angiogenesis and inhibits tumor growth. *Nat Med*. 2002;8(12):1369–1375.
23. Nair S, Boczkowski D, Moeller B, Dewhirst M, Vieweg J, Gilboa E. Synergy between tumor immunotherapy and antiangiogenic therapy. *Blood*. 2003;102(3):964–971.
24. Wada S, et al. Rationale for antiangiogenic cancer therapy with vaccination using epitope peptides derived from human vascular endothelial growth factor receptor 2. *Cancer Res*. 2005;65(11):4939–4946.
25. Wang YS, et al. Immunity against tumor angiogenesis induced by a fusion vaccine with murine beta-defensin 2 and mFlk-1. *Clin Cancer Res*. 2007; 13(22 pt 1):6779–6787.
26. Arora N, Masood R, Zheng T, Cai J, Smith DL, Gill PS. Vascular endothelial growth factor chimeric toxin is highly active against endothelial cells. *Cancer Res*. 1999;59(1):183–188.
27. Ramakrishnan S, Wild R, Nojima D. Targeting tumor vasculature using VEGF-toxin conjugates. *Methods Mol Biol*. 2001;166:219–234.
28. Millauer B, et al. Dominant-negative inhibition of Flk-1 suppresses the growth of many tumor types in vivo. *Cancer Res*. 1996;56(7):1615–1620.
29. Goldman CK, et al. Paracrine expression of a native soluble vascular endothelial growth factor receptor inhibits tumor growth, metastasis, and mortality rate. *Proc Natl Acad Sci U S A*. 1998;95(15):8795–8800.
30. Kuo CJ, et al. Comparative evaluation of the antitumor activity of antiangiogenic proteins delivered by gene transfer. *Proc Natl Acad Sci U S A*. 2001;98(8):4605–4610.
31. Spratlin JL, et al. Phase I pharmacologic and biologic study of ramucirumab (IMC-1121B), a fully human immunoglobulin G1 monoclonal antibody targeting the vascular endothelial growth factor receptor-2. *J Clin Oncol*. 2010;28(5):780–787.
32. Gattinoni L, Powell DJ Jr, Rosenberg SA, Restifo NP. Adoptive immunotherapy for cancer: building on success. *Nat Rev Immunol*. 2006;6(5):383–393.
33. Dudley ME, et al. Cancer regression and autoimmunity in patients after clonal repopulation with antitumor lymphocytes. *Science*. 2002;298(5594):850–854.
34. Dudley ME, et al. Adoptive cell transfer therapy following non-myeloablative but lymphodepleting chemotherapy for the treatment of patients with refractory metastatic melanoma. *J Clin Oncol*. 2005;23(10):2346–2357.
35. Dudley ME, et al. Adoptive cell therapy for patients with metastatic melanoma: evaluation of intensive myeloablative chemoradiation preparative regimens. *J Clin Oncol*. 2008;26(32):5233–5239.
36. Morgan RA, et al. Cancer regression in patients after transfer of genetically engineered lymphocytes. *Science*. 2006;314(5796):126–129.
37. Johnson LA, et al. Gene therapy with human and mouse T-cell receptors mediates cancer regression and targets normal tissues expressing cognate antigen. *Blood*. 2009;114(3):535–546.
38. Pule MA, et al. Virus-specific T cells engineered to coexpress tumor-specific receptors: persistence and antitumor activity in individuals with neuroblastoma. *Nat Med*. 2008;14(11):1264–1270.
39. Gattinoni L, et al. Removal of homeostatic cytokine sinks by lymphodepletion enhances the efficacy of adoptively transferred tumor-specific CD8+ T cells. *J Exp Med*. 2005;202(7):907–912.
40. North RJ. Cyclophosphamide-facilitated adoptive immunotherapy of an established tumor depends on elimination of tumor-induced suppressor T cells. *J Exp Med*. 1982;155(4):1063–1074.
41. Feng D, et al. Ultrastructural localization of the vascular permeability factor/vascular endothelial growth factor (VPF/VEGF) receptor-2 (FLK-1, KDR) in normal mouse kidney and in the hyperpermeable vessels induced by VPF/VEGF-expressing tumors and adenoviral vectors. *J Histochem Cytochem*. 2000;48(4):545–556.
42. Ran S, Huang X, Downes A, Thorpe PE. Evaluation of novel antimouse VEGFR2 antibodies as potential antiangiogenic or vascular targeting agents for tumor therapy. *Neoplasia*. 2003;5(4):297–307.
43. Simon M, et al. Expression of vascular endothelial growth factor and its receptors in human renal ontogenesis and in adult kidney. *Am J Physiol*. 1995;268(2 pt 2):F240–F250.
44. Christofori G, Naik P, Hanahan D. Vascular endothelial growth factor and its receptors, flt-1 and flk-1, are expressed in normal pancreatic islets and throughout islet cell tumorigenesis. *Mol Endocrinol*. 1995;9(12):1760–1770.
45. Lu D, et al. Tailoring in vitro selection for a picomolar affinity human antibody directed against vascular endothelial growth factor receptor 2 for enhanced neutralizing activity. *J Biol Chem*. 2003;278(44):43496–43507.
46. Ganss R, Limmer A, Sacher T, Arnold B, Hammerling GJ. Autoaggression and tumor rejection: it takes more than self-specific T-cell activation. *Immunol Rev*. 1999;169:263–272.
47. Maeurer MJ, et al. Tumor escape from immune recognition: loss of HLA-A2 melanoma cell surface expression is associated with a complex rearrangement of the short arm of chromosome 6. *Clin Cancer Res*. 1996;2(4):641–652.
48. Marincola FM, Jaffee EM, Hicklin DJ, Ferrone S. Escape of human solid tumors from T-cell recognition: molecular mechanisms and functional significance. *Adv Immunol*. 2000;74:181–273.
49. Munn DH, Mellor AL. Indoleamine 2,3-dioxygenase and tumor-induced tolerance. *J Clin Invest*. 2007;117(5):1147–1154.
50. Zou W. Immunosuppressive networks in the tumour environment and their therapeutic relevance. *Nat Rev Cancer*. 2005;5(4):263–274.
51. Niederman TM, Ghogawala Z, Carter BS, Tompkins HS, Russell MM, Mulligan RC. Antitumor activity of cytotoxic T lymphocytes engineered to target vascular endothelial growth factor receptors. *Proc Natl Acad Sci U S A*. 2002;99(10):7009–7014.
52. Huang X, et al. Combined antiangiogenic and immune therapy of prostate cancer. *Angiogenesis*. 2005;8(1):13–23.
53. Manning EA, et al. A vascular endothelial growth factor receptor-2 inhibitor enhances antitumor immunity through an immune-based mechanism. *Clin Cancer Res*. 2007;13(13):3951–3959.
54. Seavey MM, Maciag PC, Al-Rawi N, Sewell D, Paterson Y. An anti-vascular endothelial growth factor receptor 2/fetal liver kinase-1 Listeria monocytogenes anti-angiogenesis cancer vaccine for the treatment of primary and metastatic Her-2/neu+ breast tumors in a mouse model. *J Immunol*. 2009; 182(9):5537–5546.
55. Kerbel RS. A cancer therapy resistant to resistance. *Nature*. 1997;390(6658):335–336.
56. Zhang B, Karrison T, Rowley DA, Schreiber H. IFN-gamma- and TNF-dependent bystander eradication of antigen-loss variants in established mouse cancers. *J Clin Invest*. 2008;118(4):1398–1404.
57. Suzuki H, et al. VEGFR2 is selectively expressed by FOXP3high CD4+ Treg. *Eur J Immunol*. 2010;40(1):197–203.
58. Yang L, et al. Expansion of myeloid immune suppressor Gr+CD11b+ cells in tumor-bearing host directly promotes tumor angiogenesis. *Cancer Cell*. 2004;6(4):409–421.
59. Overwijk WW, et al. Tumor regression and autoimmunity after reversal of a functionally tolerant state of self-reactive CD8+ T cells. *J Exp Med*. 2003;198(4):569–580.
60. Robbins PF, et al. Cutting edge: persistence of transferred lymphocyte clonotypes correlates with cancer regression in patients receiving cell transfer therapy. *J Immunol*. 2004;173(12):7125–7130.
61. Finney HM, Akbar AN, Lawson AD. Activation of resting human primary T cells with chimeric receptors: costimulation from CD28, inducible costimulator, CD134, and CD137 in series with signals from the TCR zeta chain. *J Immunol*. 2004;172(1):104–113.
62. Wang J, et al. Optimizing adoptive polyclonal T cell immunotherapy of lymphomas, using a chimeric T cell receptor possessing CD28 and CD137 costimulatory domains. *Hum Gene Ther*. 2007;18(8):712–725.
63. Lenschow DJ, Walunas TL, Bluestone JA. CD28/B7 system of T cell costimulation. *Annu Rev Immunol*. 1996;14:233–258.
64. Friedmann-Morvinski D, Bendavid A, Waks T, Schindler D, Eshhar Z. Redirected primary T cells harboring a chimeric receptor require costimulation for their antigen-specific activation. *Blood*. 2005;105(8):3087–3093.
65. Maher J, Brentjens RJ, Gunset G, Riviere I, Sadelain M. Human T-lymphocyte cytotoxicity and proliferation directed by a single chimeric TCRzeta /CD28 receptor. *Nat Biotechnol*. 2002;20(1):70–75.

66. Zhao Y, et al. A herceptin-based chimeric antigen receptor with modified signaling domains leads to enhanced survival of transduced T lymphocytes and antitumor activity. *J Immunol*. 2009;183(9):5563–5574.
67. Bukczynski J, Wen T, Ellefsen K, Gauldie J, Watts TH. Costimulatory ligand 4-1BBL (CD137L) as an efficient adjuvant for human antiviral cytotoxic T cell responses. *Proc Natl Acad Sci U S A*. 2004;101(5):1291–1296.
68. Hurtado JC, Kim YJ, Kwon BS. Signals through 4-1BB are costimulatory to previously activated splenic T cells and inhibit activation-induced cell death. *J Immunol*. 1997;158(6):2600–2609.
69. Maus MV, et al. Ex vivo expansion of polyclonal and antigen-specific cytotoxic T lymphocytes by artificial APCs expressing ligands for the T-cell receptor, CD28 and 4-1BB. *Nat Biotechnol*. 2002; 20(2):143–148.
70. Takahashi C, Mittler RS, Vella AT. Cutting edge:4-1BB is a bona fide CD8 T cell survival signal. *J Immunol*. 1999;162(9):5037–5040.
71. Carpenito C, et al. Control of large, established tumor xenografts with genetically retargeted human T cells containing CD28 and CD137 domains. *Proc Natl Acad Sci U S A*. 2009;106(9):3360–3365.
72. Milone MC, et al. Chimeric receptors containing CD137 signal transduction domains mediate enhanced survival of T cells and increased antileukemic efficacy in vivo. *Mol Ther*. 2009;17(8):1453–1464.
73. Zhong XS, Matsushita M, Plotkin J, Riviere I, Sadelain M. Chimeric antigen receptors combining 4-1BB and CD28 signaling domains augment PI3kinase/AKT/Bcl-XL activation and CD8+ T cell-mediated tumor eradication. *Mol Ther*. 2010;18(2):413–420.
74. Dirkx AE, et al. Anti-angiogenesis therapy can overcome endothelial cell anergy and promote leukocyte-endothelium interactions and infiltration in tumors. *FASEB J*. 2006;20(6):621–630.
75. Ryden L, et al. Tumor-specific expression of vascular endothelial growth factor receptor 2 but not vascular endothelial growth factor or human epidermal growth factor receptor 2 is associated with impaired response to adjuvant tamoxifen in premenopausal breast cancer. *J Clin Oncol*. 2005; 23(21):4695–4704.
76. Heinzel FP, Sadick MD, Holaday BJ, Coffman RL, Locksley RM. Reciprocal expression of interferon gamma or interleukin 4 during the resolution or progression of murine leishmaniasis. Evidence for expansion of distinct helper T cell subsets. *J Exp Med*. 1989;169(1):59–72.
77. Reiner SL, Locksley RM. The regulation of immunity to Leishmania major. *Annu Rev Immunol*. 1995;13:151–177.
78. Kershaw MH, et al. A phase I study on adoptive immunotherapy using gene-modified T cells for ovarian cancer. *Clin Cancer Res*. 2006;12(20 pt 1):6106–6115.
79. Lamers CH, et al. Treatment of metastatic renal cell carcinoma with autologous T-lymphocytes genetically retargeted against carbonic anhydrase IX: first clinical experience. *J Clin Oncol*. 2006; 24(13):e20–e22.
80. Lamers CH, Langeveld SC, Groot-van Ruijven CM, Debets R, Sleijfer S, Gratama JW. Gene-modified T cells for adoptive immunotherapy of renal cell cancer maintain transgene-specific immune functions in vivo. *Cancer Immunol Immunother*. 2007;56(12):1875–1883.
81. Park JR, et al. Adoptive transfer of chimeric antigen receptor re-directed cytolytic T lymphocyte clones in patients with neuroblastoma. *Mol Ther*. 2007;15(4):825–833.
82. Till BG, et al. Adoptive immunotherapy for indolent non-Hodgkin lymphoma and mantle cell lymphoma using genetically modified autologous CD20-specific T cells. *Blood*. 2008;112(6):2261–2271.
83. Hanenberg H, Xiao XL, Dilloo D, Hashino K, Kato I, Williams DA. Colocalization of retrovirus and target cells on specific fibronectin fragments increases genetic transduction of mammalian cells. *Nat Med*. 1996;2(8):876–882.
84. Gao W, Rzewski A, Sun H, Robbins PD, Gambotto A. UpGene: Application of a web-based DNA codon optimization algorithm. *Biotechnol Prog*. 2004;20(2):443–448.
85. Hughes MS, et al. Transfer of a TCR gene derived from a patient with a marked antitumor response conveys highly active T-cell effector functions. *Hum Gene Ther*. 2005;16(4):457–472.
86. Onodera M, Yachie A, Nelson DM, Welchlin H, Morgan RA, Blaese RM. A simple and reliable method for screening retroviral producer clones without selectable markers. *Hum Gene Ther*. 1997;8(10):1189–1194.
87. Kochenderfer JN, et al. Construction and preclinical evaluation of an anti-CD19 chimeric antigen receptor. *J Immunother*. 2009;32(7):689–702.